

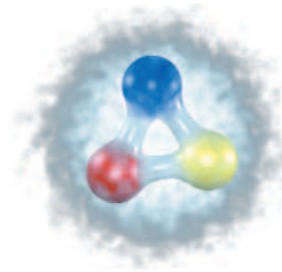
# Bonn-Gatchina partial wave analysis

**A. Sarantsev**

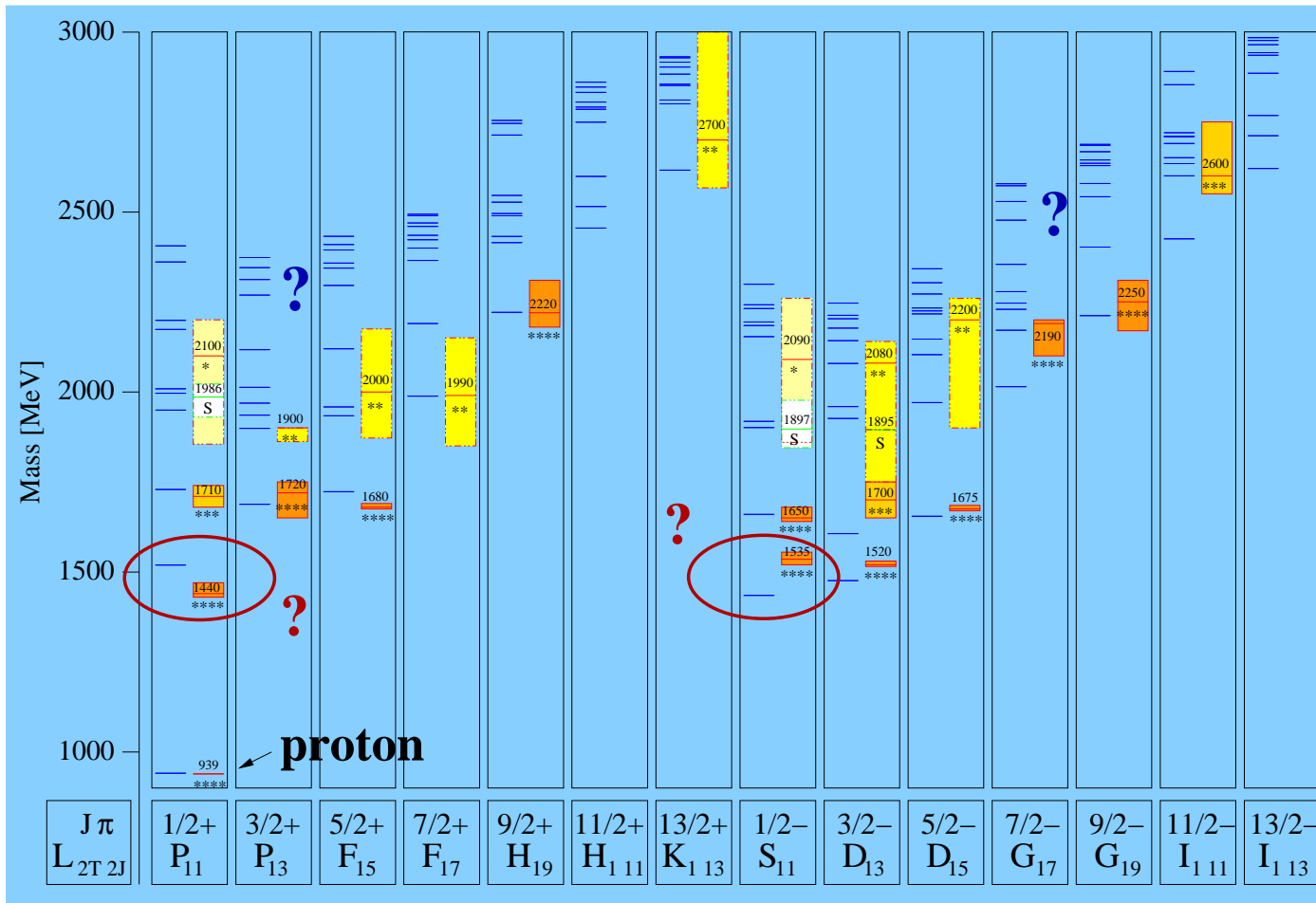
**HISKP, Uni-Bonn (Bonn) and PNPI (Gatchina)**

# $N^*$ - resonances in the quark model

Nukleon  
 $10^{-15}$  m



U. Loering, B. Metsch, H. Petry et al. (Bonn)



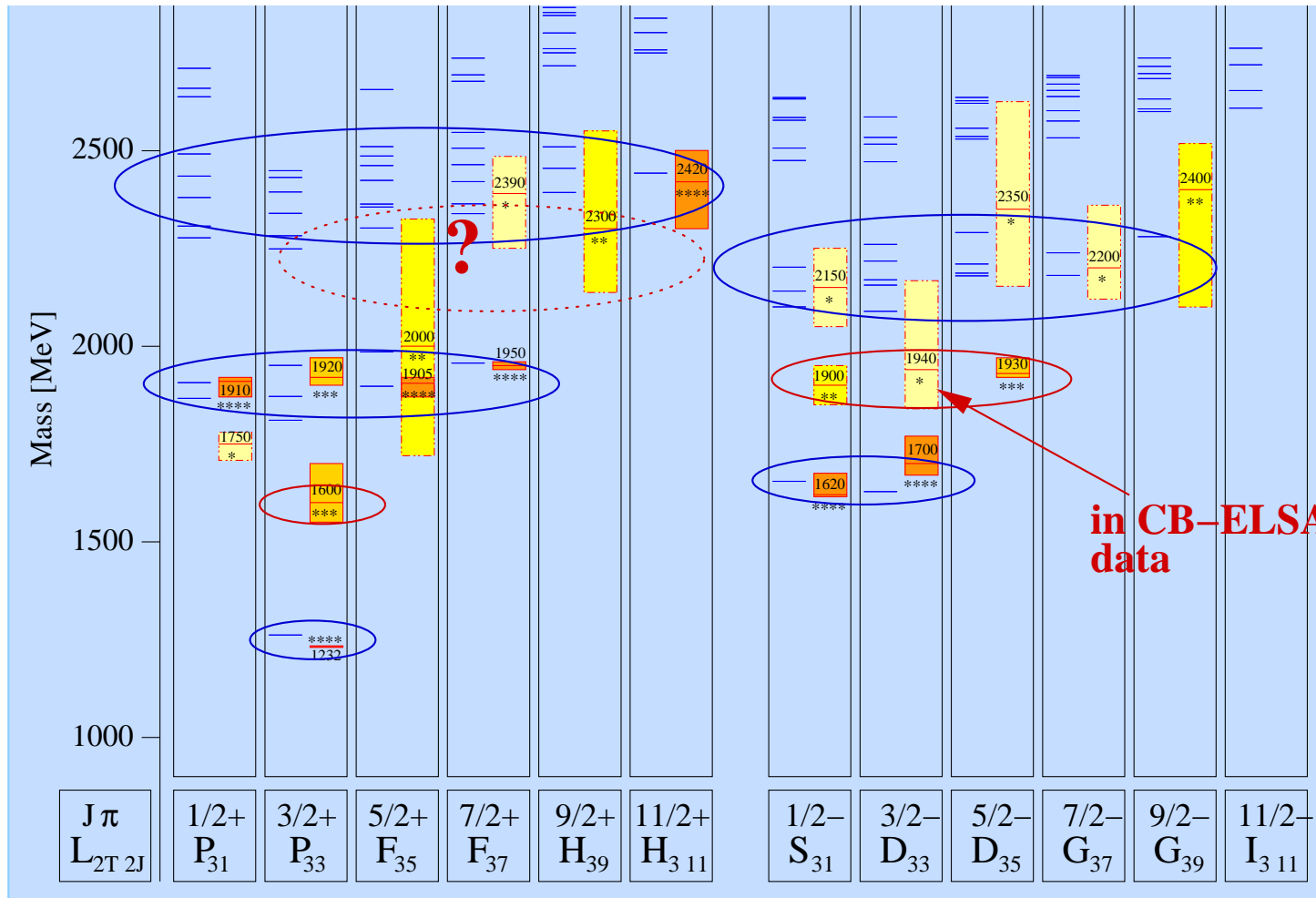
↔

Constituent quarks

Confinement-potential

Residual interaction

# The $\Delta^*$ - states



Quark model  
U. Löring, B. Metsch,  
H. Petry et al.

model  
 $\sim 2n + l$

data  
 $\sim n + l ?$

$\leftrightarrow$  Parity  
doublets ?

$\leftrightarrow$  Additional experimental information needed !!

## Bonn-Gatchina PWA group

A. Anisovich, E. Klempt, V. Nikonov, A. Sarantsev and U. Thoma.

**1. The P-vector based analysis of single and multi-meson photoproduction data.**

The combined analysis of CB-ELSA data on  $\gamma p \rightarrow \pi^0 p$ ,  $\gamma p \rightarrow \eta p$ ,  $\gamma p \rightarrow \pi^0 \pi^0 p$ ,  $\gamma p \rightarrow \pi^0 \eta p$ ,  $\gamma n \rightarrow \eta n$ ,  $\gamma n \rightarrow \pi^0 n$  and  $\gamma p \rightarrow \omega p$  with data from other collaborations: CLAS, GRAAL, LEPS.

**2. The K-matrix analysis of pion-induced data on the reactions  $\pi N \rightarrow \pi N$  (on the basis of SAID energy-fixed partial wave analysis),  $\pi p \rightarrow \pi^0 \pi^0 n$  and recently included:  $\pi p \rightarrow \eta n$ ,  $\pi^- p \rightarrow K^0 \Lambda$  and  $\pi^+ p \rightarrow K^+ \Sigma$ .**

**3. Analysis of  $NN$  interaction. The analysis of  $pp \rightarrow K \Lambda p$  data and analysis of the  $pp \rightarrow \pi^0 p$  and  $np \rightarrow pp\pi^-$  data.**

The fitted reactions. **Recently included data sets.** **New points added**

Observable	$N_{\text{data}}$	$\frac{\chi^2}{N_{\text{data}}}$		Observable	$N_{\text{data}}$	$\frac{\chi^2}{N_{\text{data}}}$	
$\sigma(\gamma p \rightarrow p\pi^0)$	<b>1106</b>	<b>1.27</b>	<b>CB-ELSA</b>	$\sigma(\gamma p \rightarrow p\pi^0)$	<b>861</b>	<b>1.74</b>	<b>GRAAL</b>
$\sigma(\frac{3}{2} - \frac{1}{2})(p\pi^0)$	<b>140</b>	<b>1.41</b>	<b>A2GDH</b>	$\Sigma(\gamma p \rightarrow p\pi^0)$	<b>1492</b>	<b>3.38</b>	<b>SAID</b>
$P(\gamma p \rightarrow p\pi^0)$	<b>607</b>	<b>3.16</b>	<b>SAID</b>	$T(\gamma p \rightarrow p\pi^0)$	<b>389</b>	<b>4.01</b>	<b>SAID</b>
$H(\gamma p \rightarrow p\pi^0)$	<b>71</b>	<b>1.92</b>	<b>SAID</b>	$G(\gamma p \rightarrow p\pi^0)$	<b>75</b>	<b>2.58</b>	<b>SAID</b>
$Ox(\gamma p \rightarrow p\pi^0)$	<b>7</b>	<b>1.01</b>	<b>SAID</b>	$Oz(\gamma p \rightarrow p\pi^0)$	<b>7</b>	<b>0.38</b>	<b>SAID</b>
$\sigma(\gamma p \rightarrow n\pi^+)$	<b>1583</b>	<b>1.87</b>	<b>SAID</b>	$\sigma(\gamma p \rightarrow n\pi^+)$	<b>408</b>	<b>2.09</b>	<b>A2GDH</b>
$\Sigma(\gamma p \rightarrow n\pi^+)$	<b>899</b>	<b>4.23</b>	<b>SAID</b>	$\sigma(\frac{3}{2} - \frac{1}{2})(n\pi^+)$	<b>231</b>	<b>2.49</b>	<b>A2GDH</b>
$P(\gamma p \rightarrow n\pi^+)$	<b>252</b>	<b>3.90</b>	<b>SAID</b>	$T(\gamma p \rightarrow n\pi^+)$	<b>661</b>	<b>3.66</b>	<b>SAID</b>
$H(\gamma p \rightarrow p\pi^0)$	<b>71</b>	<b>1.92</b>	<b>SAID</b>	$G(\gamma p \rightarrow p\pi^0)$	<b>75</b>	<b>2.58</b>	<b>SAID</b>
$S_{11}(\pi N \rightarrow \pi N)$	<b>126</b>	<b>1.40</b>	<b>SAID</b>	$P_{11}(\pi N \rightarrow \pi N)$	<b>110</b>	<b>2.24</b>	<b>SAID</b>
$P_{13}(\pi N \rightarrow \pi N)$	<b>108</b>	<b>2.57</b>	<b>SAID</b>	$P_{33}(\pi N \rightarrow \pi N)$	<b>130</b>	<b>4.56</b>	<b>SAID</b>
$D_{33}(\pi N \rightarrow \pi N)$	<b>136</b>	<b>4.51</b>	<b>SAID</b>	$D_{13}(\pi N \rightarrow \pi N)$	<b>106</b>	<b>5.06</b>	<b>SAID</b>
$\sigma(\gamma p \rightarrow p\eta)$	<b>667</b>	<b>0.92</b>	<b>CB-ELSA</b>	$\sigma(\gamma p \rightarrow p\eta)$	<b>100</b>	<b>2.72</b>	<b>TAPS</b>
$\Sigma(\gamma p \rightarrow p\eta)$	<b>51</b>	<b>2.06</b>	<b>GRAAL 98</b>	$\Sigma(\gamma p \rightarrow p\eta)$	<b>100</b>	<b>2.01</b>	<b>GRAAL 04</b>
$T(\gamma p \rightarrow p\eta)$	<b>50</b>	<b>1.52</b>	<b>Phoenixis</b>	$\sigma(\pi^- p \rightarrow n\eta)$	<b>288</b>	<b>2.76</b>	<b>CBALL+Richards</b>

The fitted reactions. **Recently included data sets.**

Observable	$N_{\text{data}}$	$\frac{\chi^2}{N_{\text{data}}}$		Observable	$N_{\text{data}}$	$\frac{\chi^2}{N_{\text{data}}}$	
$C_x(\gamma p \rightarrow \Lambda K^+)$	160	1.22	CLAS	$C_x(\gamma p \rightarrow \Sigma^0 K^+)$	94	2.29	CLAS
$C_z(\gamma p \rightarrow \Lambda K^+)$	160	1.53	CLAS	$C_z(\gamma p \rightarrow \Sigma^0 K^+)$	94	2.19	CLAS
$\sigma(\gamma p \rightarrow \Lambda K^+)$	1377	1.80	CLAS	$\sigma(\gamma p \rightarrow \Sigma^0 K^+)$	1280	2.68	CLAS
$P(\gamma p \rightarrow \Lambda K^+)$	202	2.31	CLAS	$P(\gamma p \rightarrow \Sigma^0 K^+)$	95	1.56	CLAS
$\Sigma(\gamma p \rightarrow \Lambda K^+)$	66	2.70	GRAAL	$\Sigma(\gamma p \rightarrow \Sigma^0 K^+)$	42	0.67	GRAAL
$\Sigma(\gamma p \rightarrow \Lambda K^+)$	45	1.75	LEP	$\Sigma(\gamma p \rightarrow \Sigma^0 K^+)$	45	1.03	LEP
$T(\gamma p \rightarrow \Lambda K^+)$	66	2.11	GRAAL	$\sigma(\gamma p \rightarrow \Sigma^+ K^0)$	48	3.36	CLAS
$Ox(\gamma p \rightarrow \Lambda K^+)$	66	1.40	GRAAL	$\sigma(\gamma p \rightarrow \Sigma^+ K^0)$	160	0.95	CB-ELSA
$Oz(\gamma p \rightarrow \Lambda K^+)$	66	1.86	GRAAL	$P(\gamma p \rightarrow \Sigma^+ K^0)$	72	0.72	CB-ELSA
$\sigma(\gamma p \rightarrow p\pi^0\pi^0)$	CB-ELSA (1.4 GeV)			$E(\gamma p \rightarrow p\pi^0\pi^0)$	16	2.08	MAMI
$\sigma(\gamma p \rightarrow p\pi^0\eta)$	CB-ELSA (3.2 GeV)			$\Sigma(\gamma p \rightarrow p\pi^0\eta)$	180	2.68	GRAAL
$\sigma(\gamma p \rightarrow p\pi^0\pi^0)$	CB-ELSA (3.2 GeV)			$\Sigma(\gamma p \rightarrow p\pi^0\pi^0)$	128	0.85	GRAAL
$\sigma(\pi^- p \rightarrow K\Lambda)$	479	1.55	RAL	$P(\pi^- p \rightarrow K\Lambda)$	261	1.76	RAL+ANL
$\sigma(\pi^+ p \rightarrow K^+\Sigma)$	609	1.91	RAL	$P(\pi^+ p \rightarrow K^+\Sigma)$	420	2.74	RAL

## Combined analysis of the different reactions:

For pion induced reactions the transition partial wave amplitude can be written as:

$$A_{1i} = K_{1j}(I - i\rho K)_{ji}^{-1}$$

and

$$K_{ij} = \sum_{\alpha} \frac{g_i^{\alpha} g_j^{\alpha}}{M_{\alpha}^2 - s} + f_{ij}(s)$$

where  $f_{ij}$  is nonresonant transition part.

For the photoproduction:

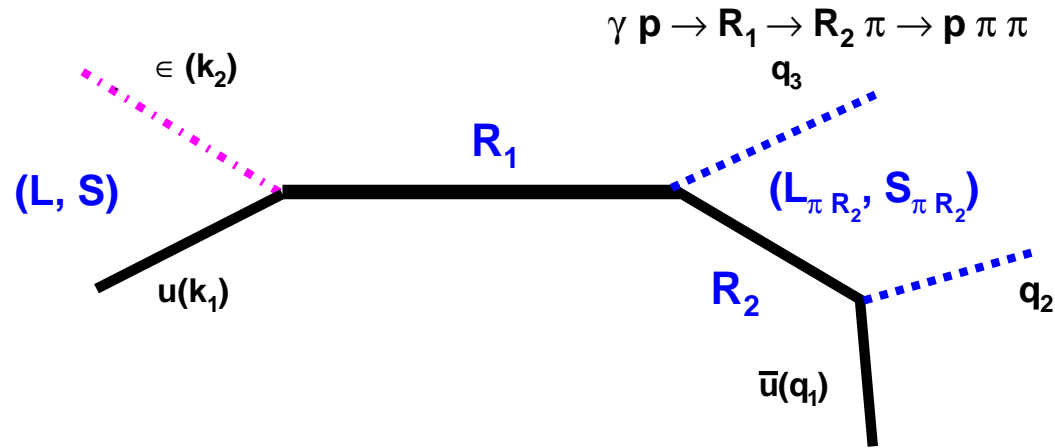
$$A_k = P_j(I - i\rho K)_{jk}^{-1}$$

The vector of the initial interaction has the form:

$$P_j = \sum_{\alpha} \frac{\Lambda_i^{\alpha} g_j^{\alpha}}{M_{\alpha}^2 - s} + F_j(s)$$

Here  $F_j$  is nonresonant production of the final state  $j$ .

# The resonance amplitudes for meson photoproduction



The general form of the angular dependent part of the amplitude:

$$\bar{u}(q_1) \tilde{N}_{\alpha_1 \dots \alpha_n} (R_2 \rightarrow \mu N) F_{\beta_1 \dots \beta_n}^{\alpha_1 \dots \alpha_n} (q_1 + q_2) \tilde{N}_{\gamma_1 \dots \gamma_m}^{(j) \beta_1 \dots \beta_n} (R_1 \rightarrow \mu R_2) \\ F_{\xi_1 \dots \xi_m}^{\gamma_1 \dots \gamma_m} (P) V_{\xi_1 \dots \xi_m}^{(i) \mu} (R_1 \rightarrow \gamma N) u(k_1) \varepsilon_\mu$$

$$F_{\nu_1 \dots \nu_L}^{\mu_1 \dots \mu_L} (p) = (m + \hat{p}) O_{\alpha_1 \dots \alpha_L}^{\mu_1 \dots \mu_L} \frac{L+1}{2L+1} \left( g_{\alpha_1 \beta_1}^\perp - \frac{L}{L+1} \sigma_{\alpha_1 \beta_1} \right) \prod_{i=2}^L g_{\alpha_i \beta_i} O_{\nu_1 \dots \nu_L}^{\beta_1 \dots \beta_L}$$

$$\sigma_{\alpha_i \alpha_j} = \frac{1}{2} (\gamma_{\alpha_i} \gamma_{\alpha_j} - \gamma_{\alpha_j} \gamma_{\alpha_i})$$

The Reggeized  $t$ - and  $u$ - channel exchanges can be projected to the s-channel.

$$J_\mu = i\mathcal{F}_1\sigma_\mu + \mathcal{F}_2(\vec{\sigma}\vec{q})\frac{\varepsilon_{\mu ij}\sigma_i k_j}{|\vec{k}||\vec{q}|} + i\mathcal{F}_3\frac{(\vec{\sigma}\vec{k})}{|\vec{k}||\vec{q}|}q_\mu + i\mathcal{F}_4\frac{(\vec{\sigma}\vec{q})}{\vec{q}^2}q_\mu .$$

the multipoles can be reconstructed as:

$$\begin{aligned} E_n^+ &= \frac{1}{n+1} \int \frac{dz}{2} \left[ \mathcal{F}_1 P_n(z) - \mathcal{F}_2 P_{n+1}(z) + \mathcal{F}_3 \frac{1-z^2}{(n+1)} P'_n(z) + \mathcal{F}_4 \frac{1-z^2}{(n+2)} P'_{n+1}(z) \right] \\ M_n^+ &= \frac{1}{n+1} \int \frac{dz}{2} \left[ \mathcal{F}_1 P_n(z) - \mathcal{F}_2 P_{n+1}(z) - \mathcal{F}_3 \frac{1-z^2}{n(n+1)} P'_n(z) \right] \\ E_n^- &= \int \frac{dz}{2} \frac{(n+1)^2(n+2)}{2n+1} [-\mathcal{F}_1 P_{n+1}(z) + \mathcal{F}_2 P_n(z)] + \\ &\quad \int \frac{dz}{2} \frac{2(2n-1)(1-z^2)}{(2n+1)(2n-3)} \left[ \mathcal{F}_3 P'_{n+1}(z) + \frac{(n+2)}{n(2n-3)} \mathcal{F}_4 P'_n(z) \right] \\ M_n^- &= \int \frac{dz}{2} \frac{(n+1)^2(n+2)}{2n+1} \left[ \mathcal{F}_1 P_{n+1}(z) - \mathcal{F}_2 P_n(z) \right] + \frac{(1-z^2)}{(2n+1)} \mathcal{F}_3 P'_{n+1}(z) \end{aligned}$$

# $\gamma p \rightarrow \pi^0 p$ from Crystal Barrel at ELSA ( $E_\gamma \leq 3.2$ GeV)

$\Delta(1232)P_{33}$

$N(1520)D_{13} S_{11}$

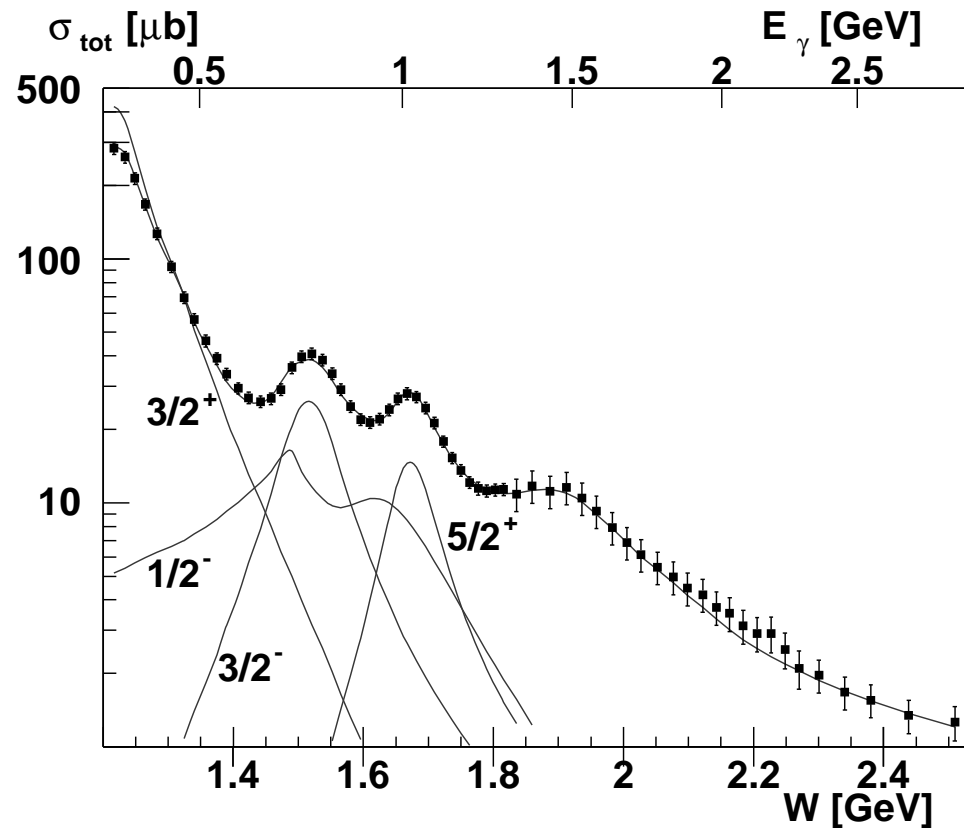
$N(1680)F_{15}$

$\Delta(1700)D_{33}$

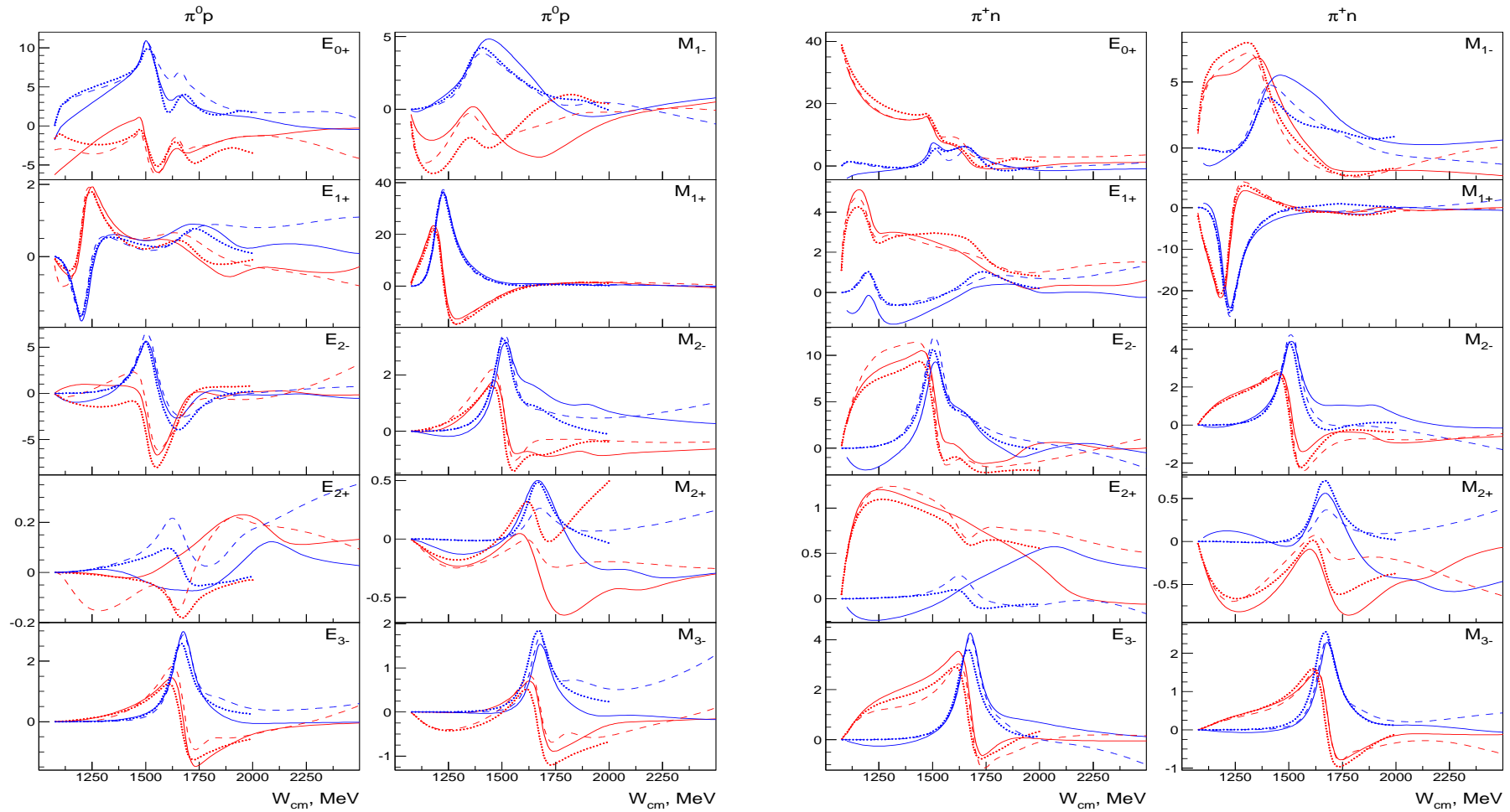
$\Delta(1920)P_{33}$

**Non-resonance contribution:**

**t-channel  $\rho - \omega$  exchange,  
u-exchange and non-  
resonance production in  
 $J^P = 3/2^+$  wave**



The multipoles for single pion production. **Red - real part, Blue - imaginary part.** Solid curves BoGa -solution, dashed curves - SAID solution, dotted - MAID 2009.



# $\gamma p \rightarrow \eta p$ from Crystal Barrel at ELSA ( $E_\gamma \leq 3.2$ GeV)

Main resonance contributions:

$N(1535)S_{11}$

$N(1650)S_{11}$

$N(1720)P_{13}$

**new**  $N(2070)D_{15}$

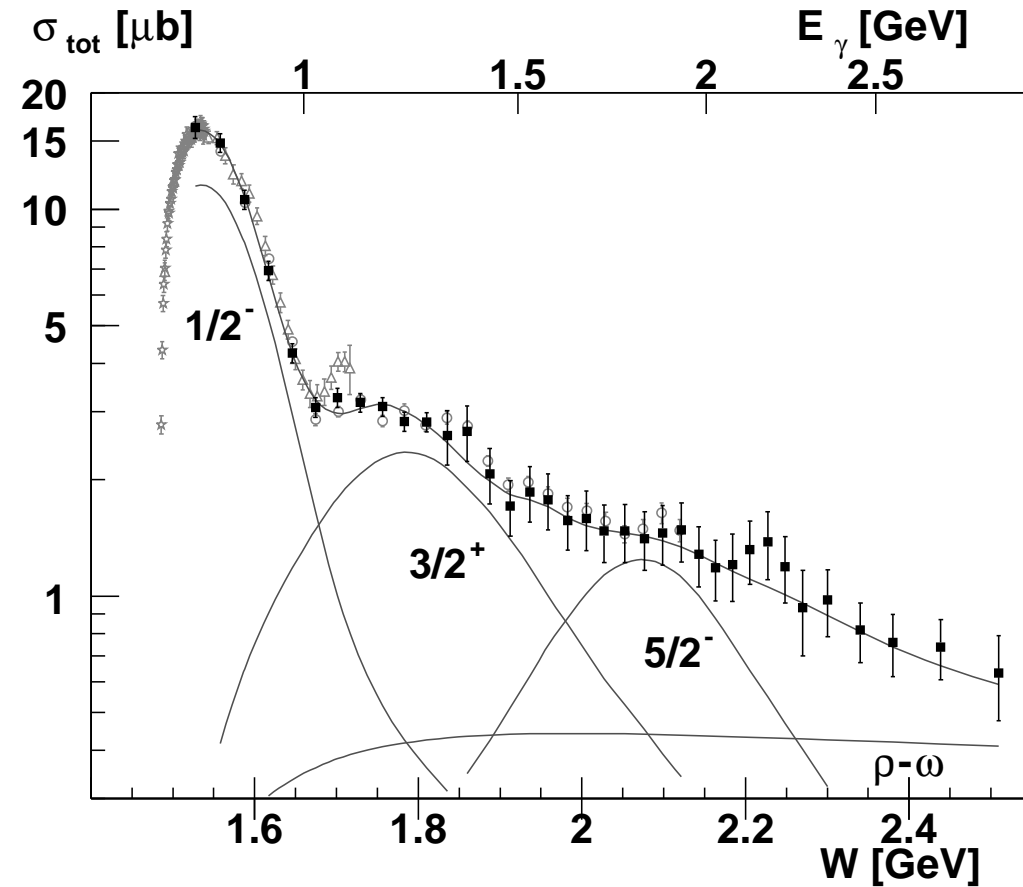
Non-resonance contribution:

reggeized t-channel

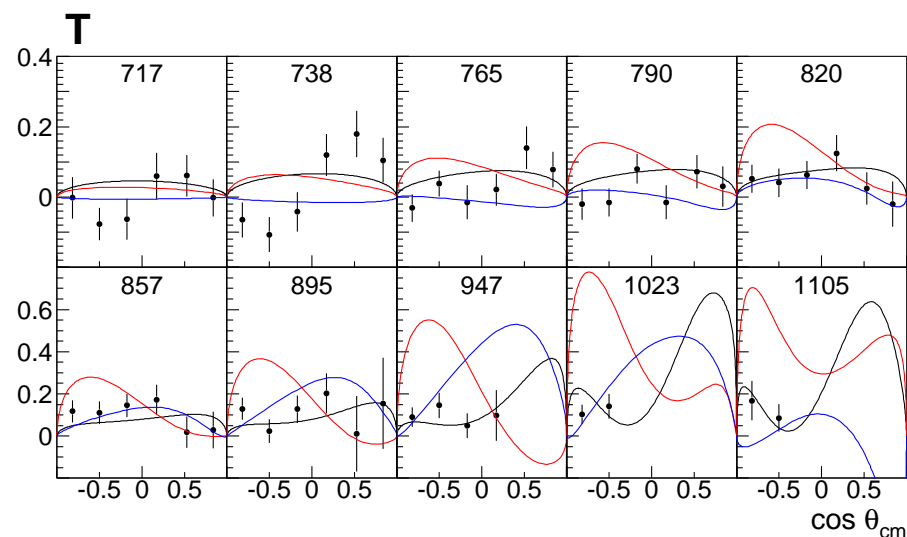
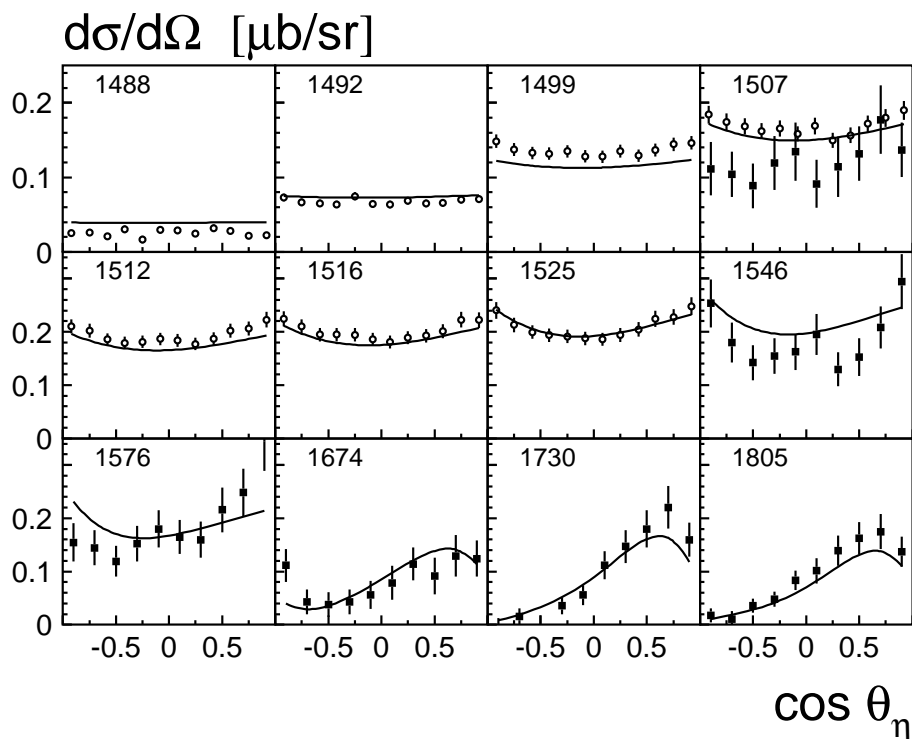
$\rho - \omega$  exchange.

**No evidence for third**

$N(1800)S_{11}$

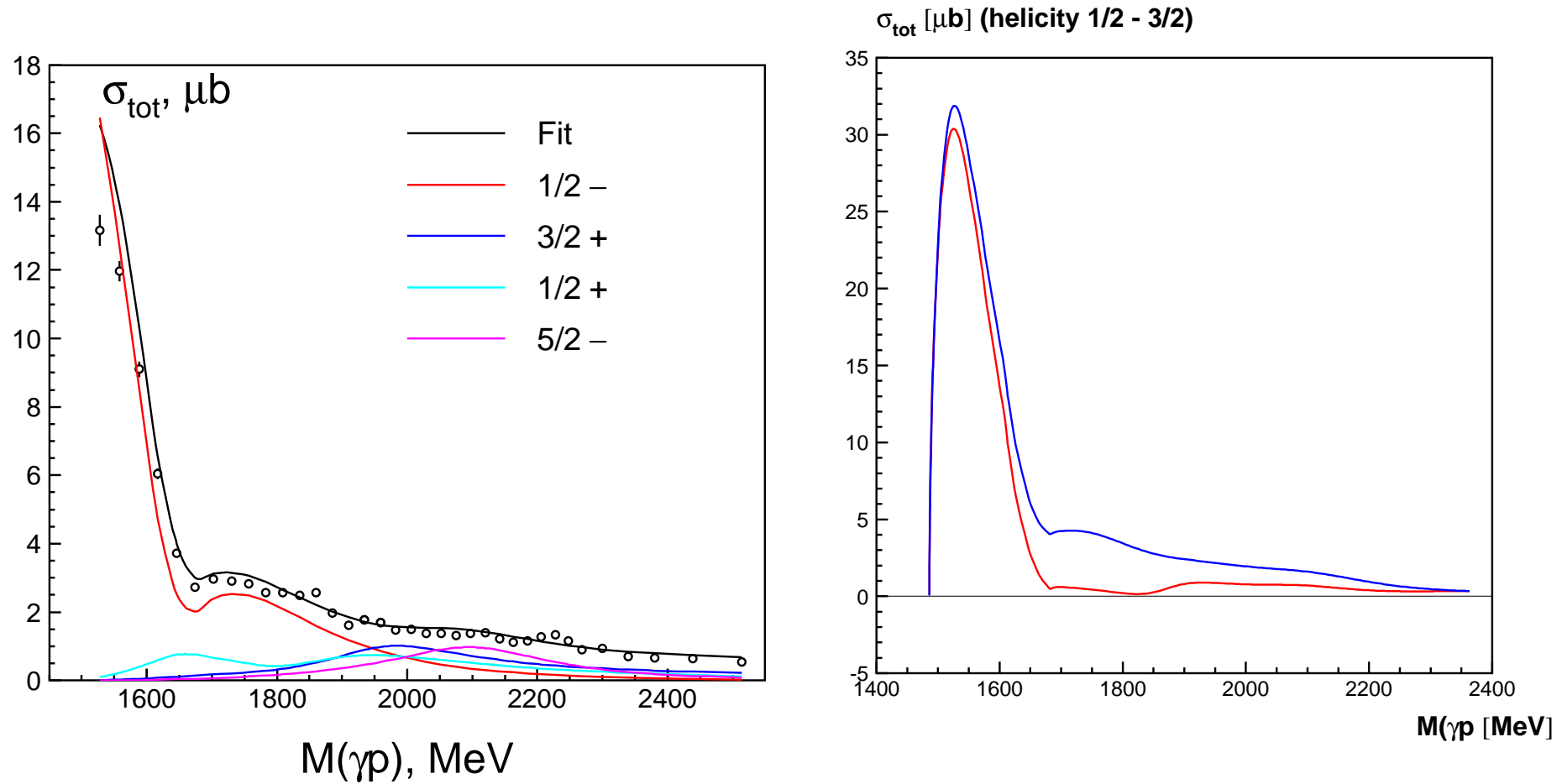


The data on  $\pi^- p \rightarrow \eta n$  and the target asymmetry  $\gamma p \rightarrow \eta p$  fix the position and couplings of  $P_{11}(1710)$  state and reduce  $\eta N$  coupling of the  $P_{13}(1720)$  state.



Observable	$N_{\text{data}}$	$\frac{\chi^2}{N_{\text{data}}}$		Observable	$N_{\text{data}}$	$\frac{\chi^2}{N_{\text{data}}}$	
$\sigma(\gamma p \rightarrow p\eta)$	667	0.92 (0.85)	CB-ELSA	$\sigma(\gamma p \rightarrow p\eta)$	100	2.72 (1.97)	TAPS
$\Sigma(\gamma p \rightarrow p\eta)$	51	2.06 (1.81)	GRAAL 98	$\Sigma(\gamma p \rightarrow p\eta)$	100	2.01 (1.43)	GRAAL 04

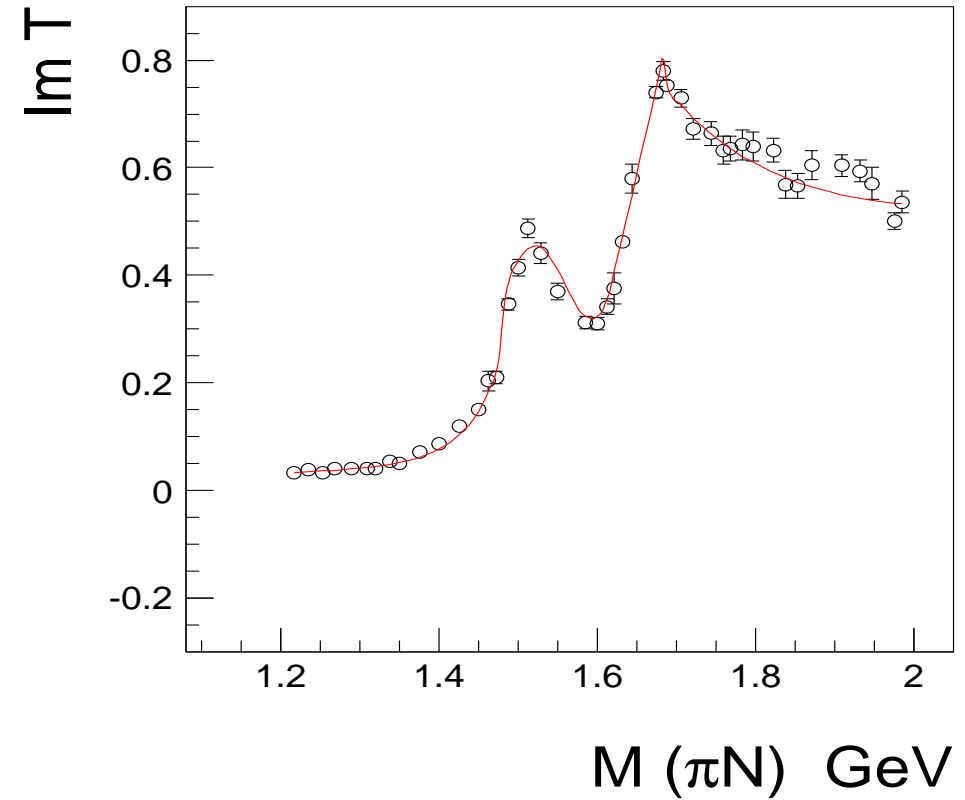
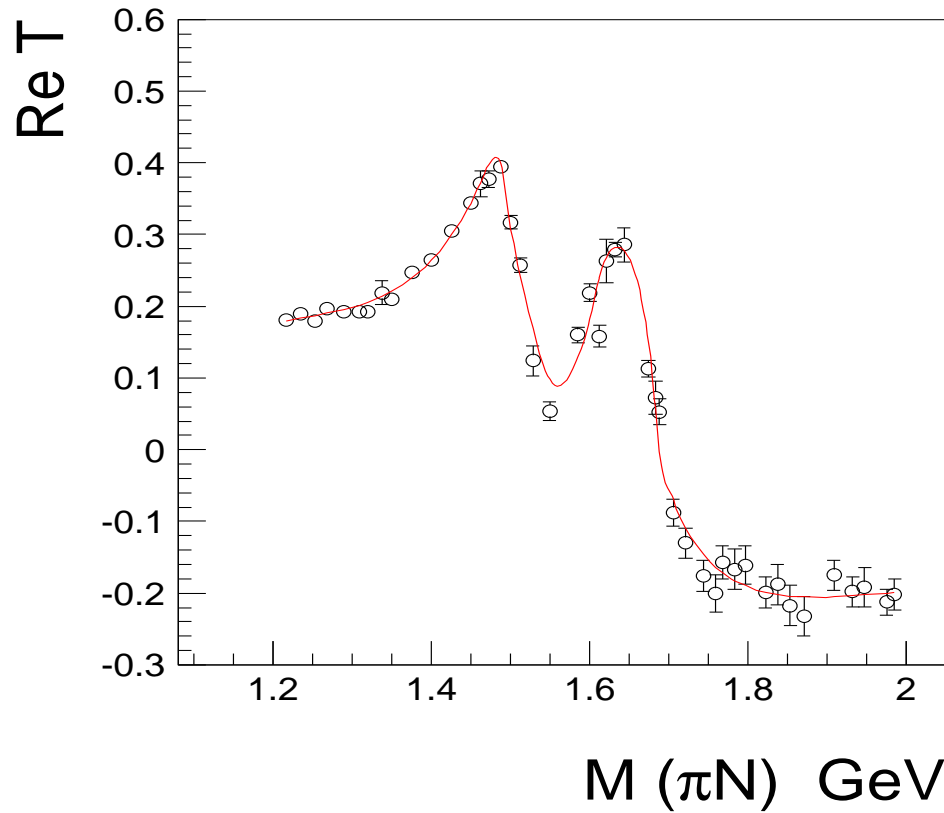
The target asymmetry  $\gamma p \rightarrow \eta p$  data reduce coupling of the  $P_{13}(1720)$  state to the  $\eta N$  channel by factor  $\sim 1.7$ .



$N\pi \rightarrow N\pi$ ,  $S_{11}$  wave (2 pole 5 channel K-matrix)

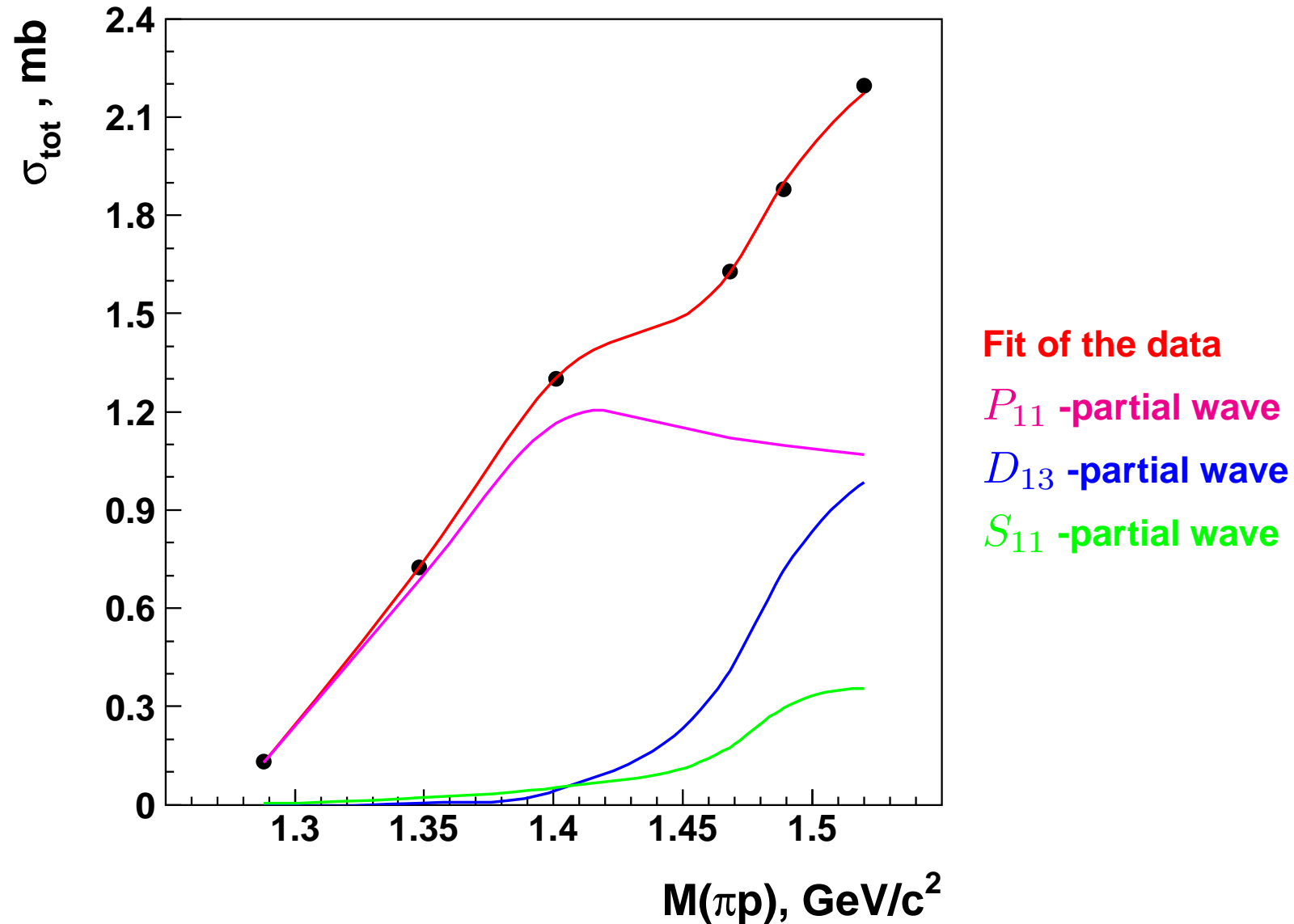
$S_{11}$

$S_{11}$



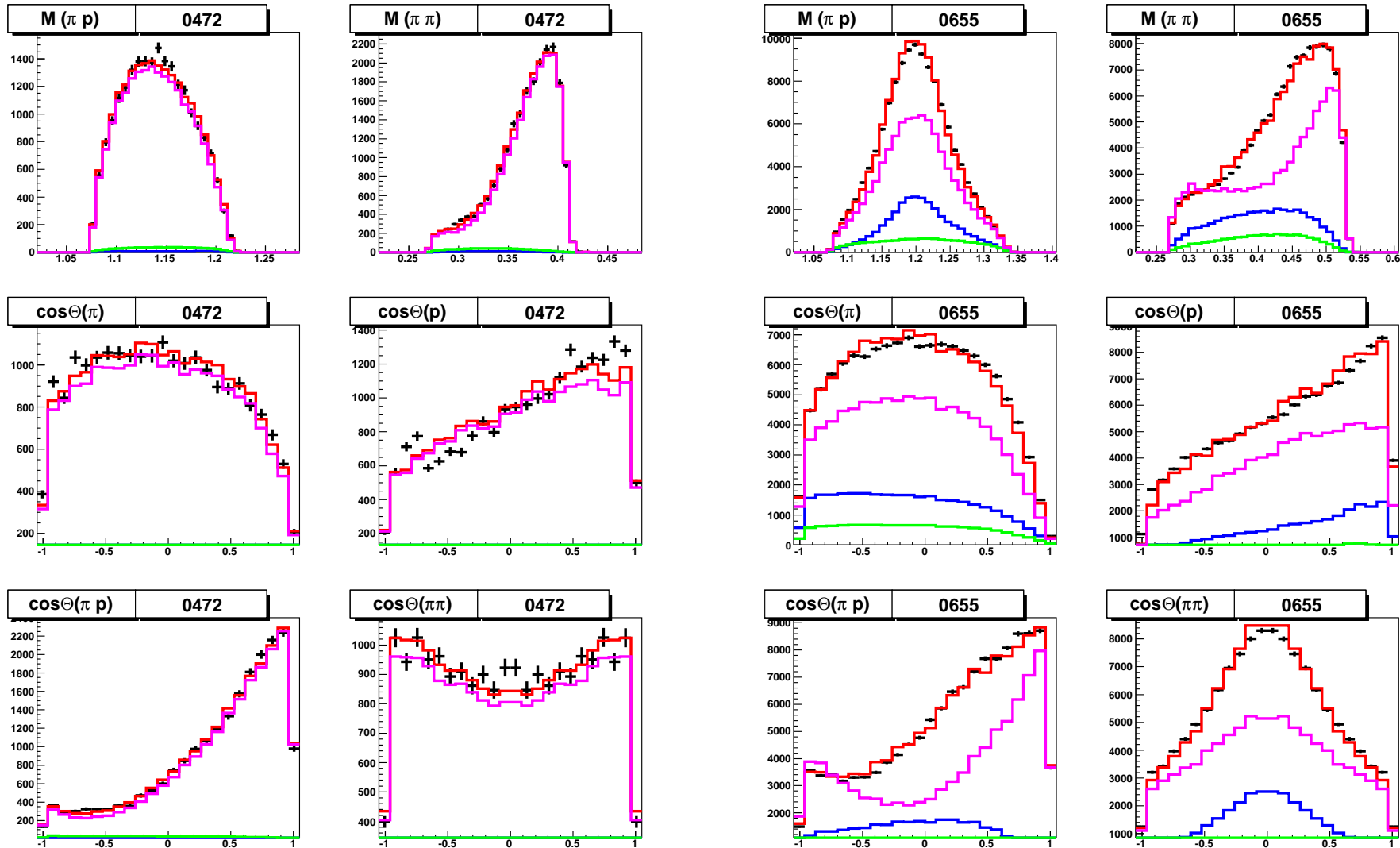
**T-matrix poles:**  $M = 1508_{-30}^{+10}$  MeV,  $2 Im = 165 \pm 15$  MeV;

$M = 1645 \pm 15$  MeV,  $2 Im = 187 \pm 20$  MeV

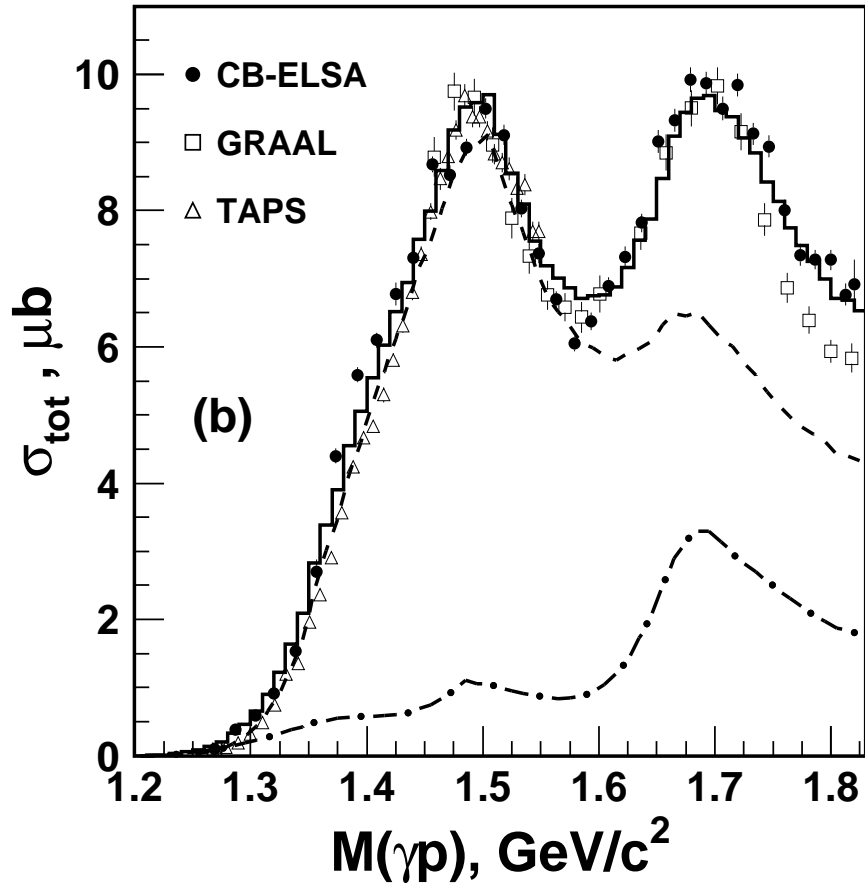
$\pi^- p \rightarrow n\pi^0\pi^0$  (Crystal Ball) total cross section

# $\pi^- p \rightarrow n \pi^0 \pi^0$ (Crystal Ball)

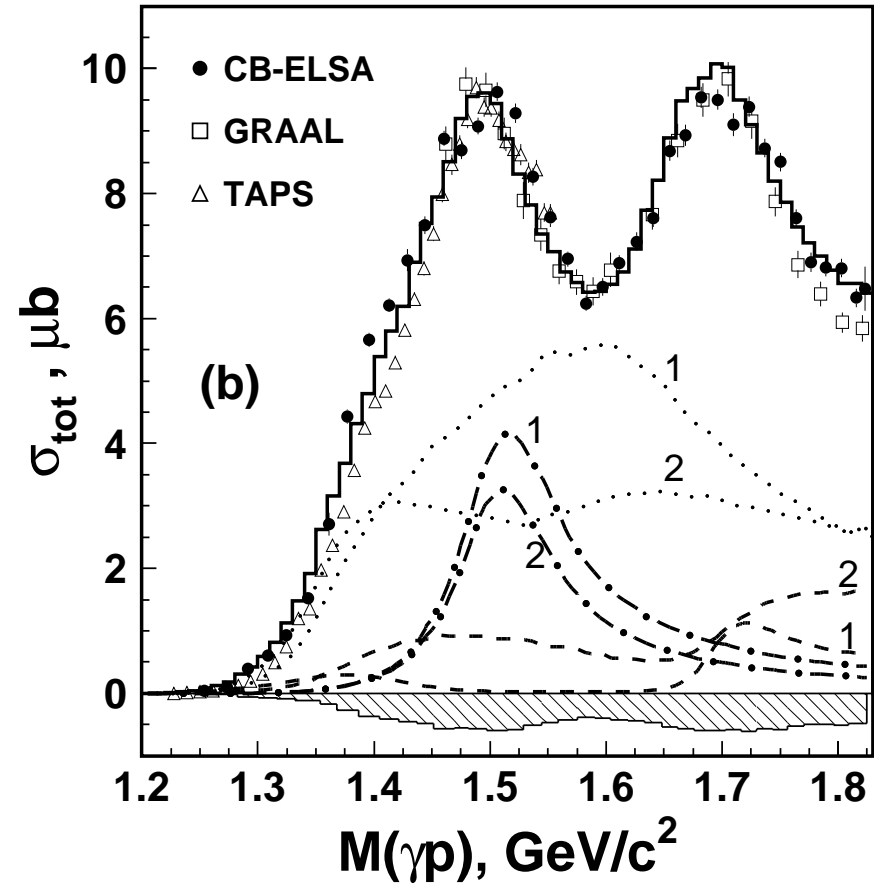
Differential cross sections for 472 and 665 MeV/c data.



$\gamma p \rightarrow p\pi^0\pi^0$  (CB-ELSA) M.Fuchs et al.



PWA corrected cross section and contributions from  $\Delta(1232)\pi$  (dashed) and  $N\sigma$  (dashed-dotted) final states.



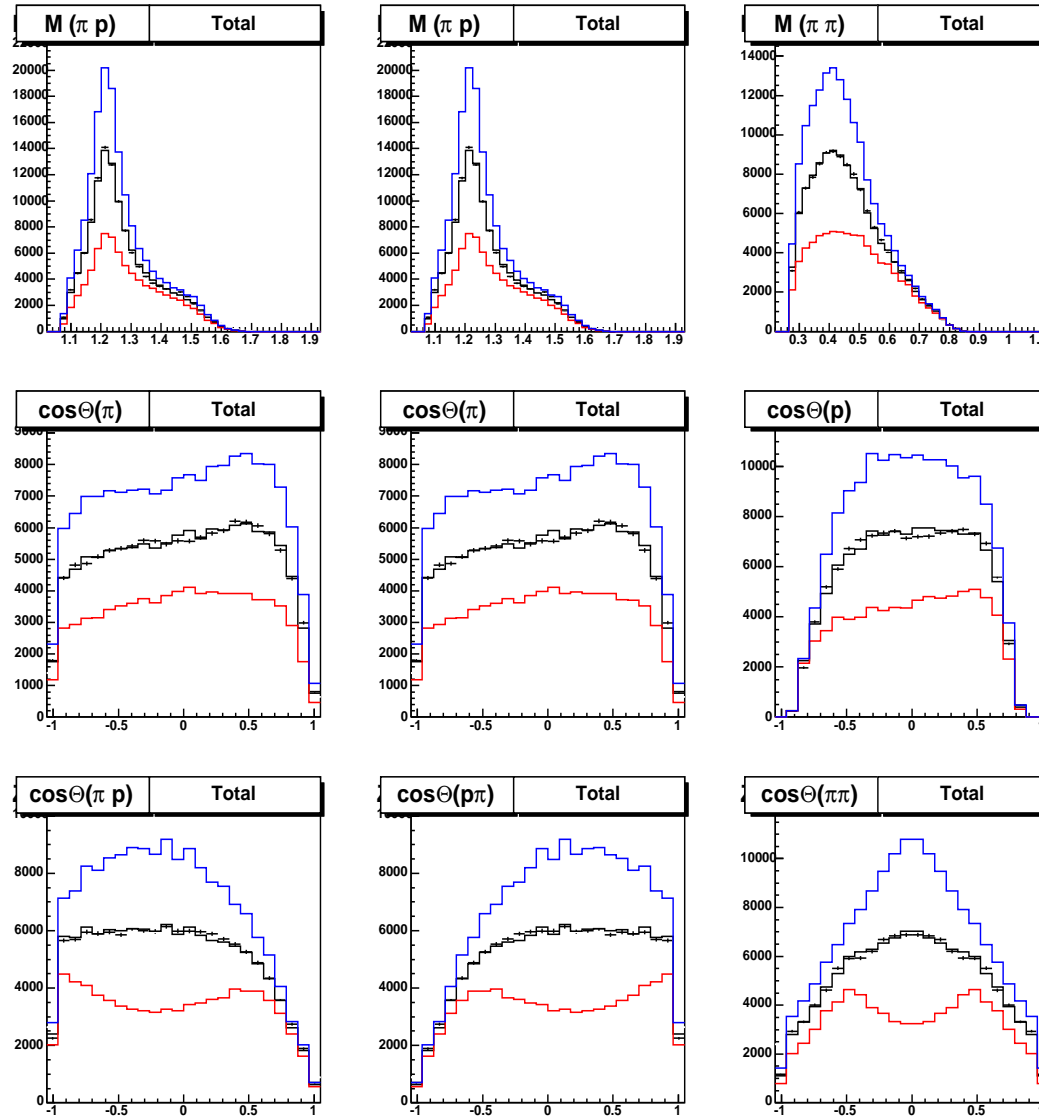
Contributions from  $D_{33}$  (dotted),  $P_{11}$  (dashed) and  $D_{13}$  (dashed-dotted) partial waves.

The  $\gamma p \rightarrow \pi^0 \pi^0 p$  differential cross section for the total energy region.

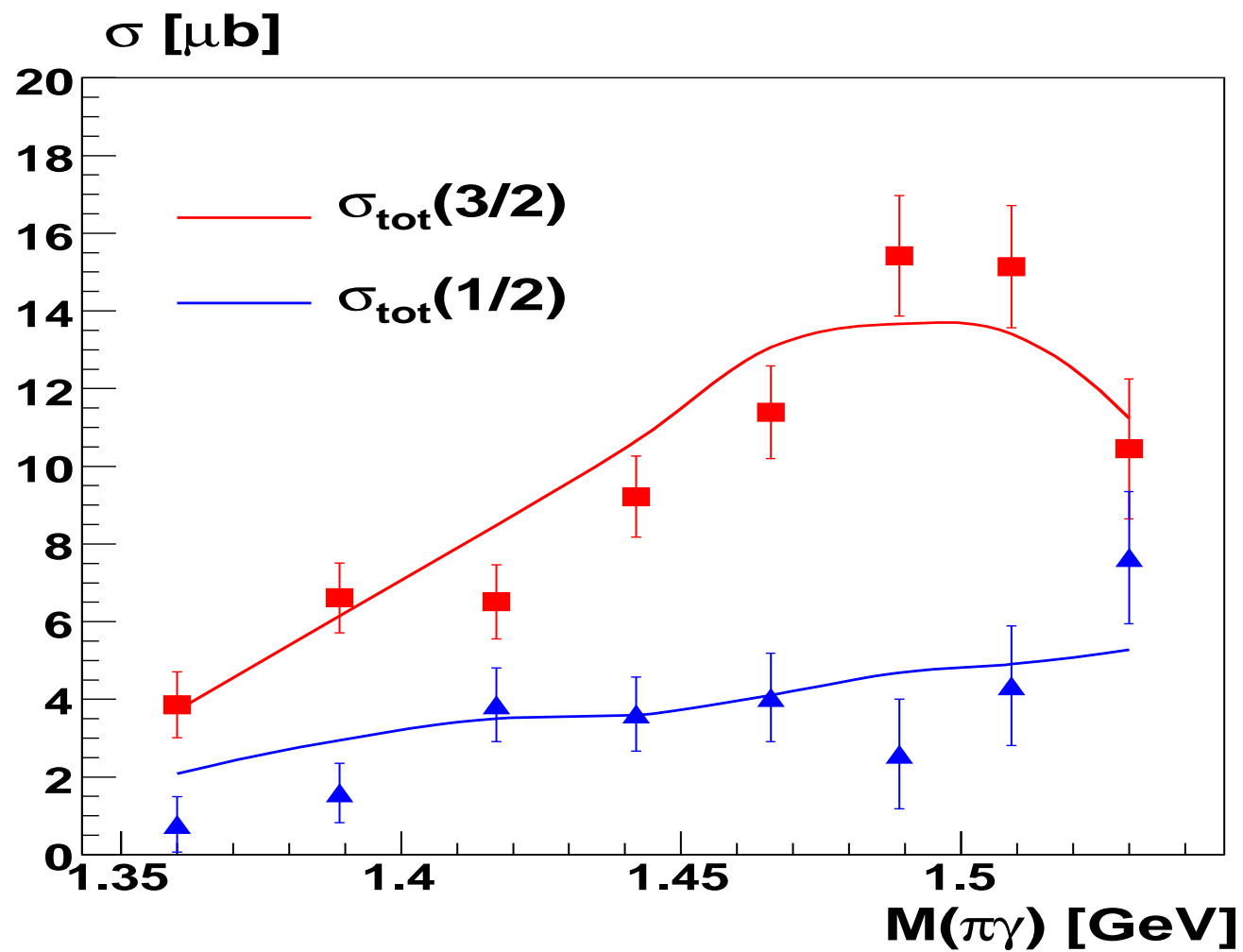
The fit of the unpolarized data and prediction for the double polarization measurements.

Red curve: only helicity 1/2 amplitudes contributed to the cross section.

Blue curve: only helicity 3/2 amplitudes.



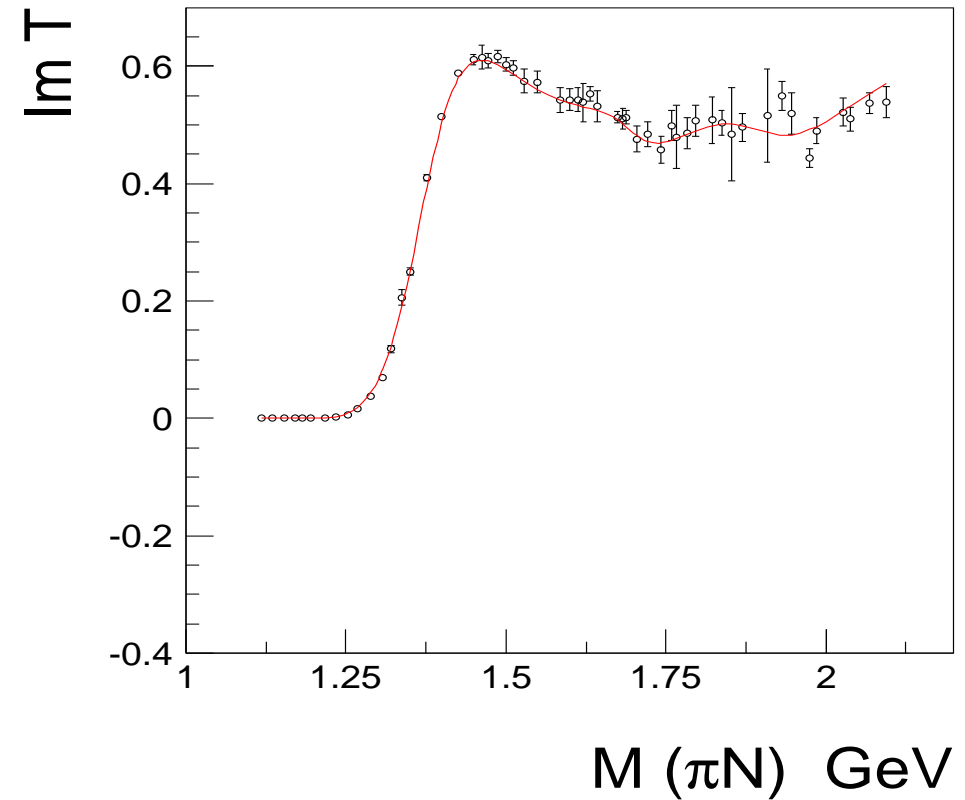
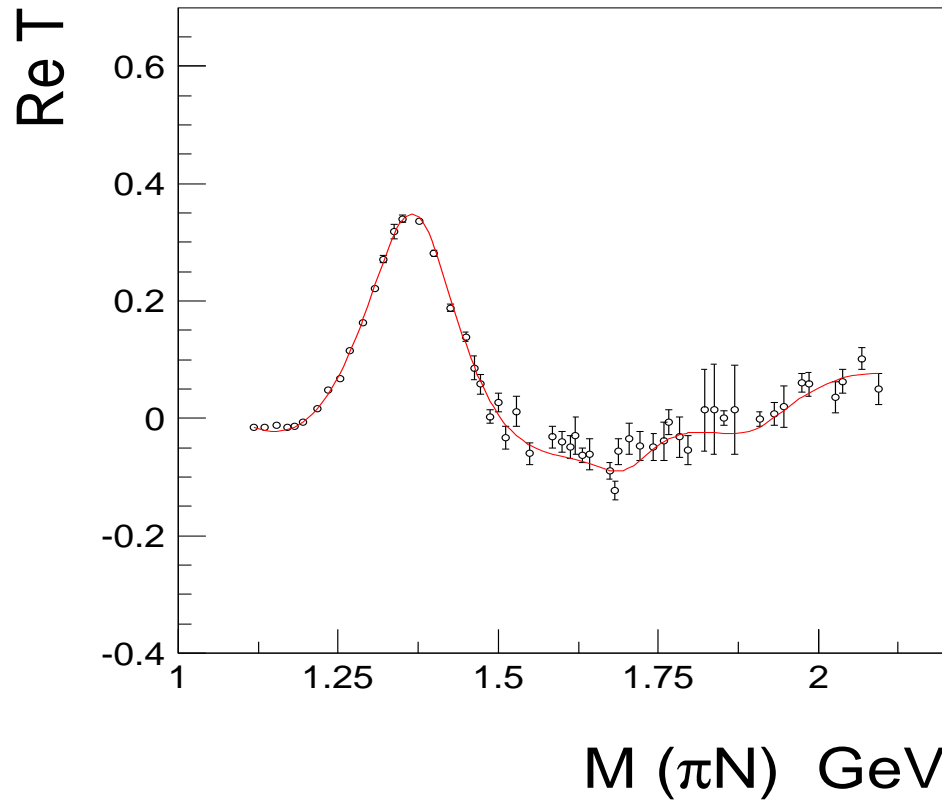
The  $\gamma p \rightarrow \pi^0 \pi^0 p$  helicity 3/2 and 1/2 differential cross sections



# $N\pi \rightarrow N\pi P_{11}$ wave (3 pole 4 channel K-matrix)

$P_{11}$

$P_{11}$

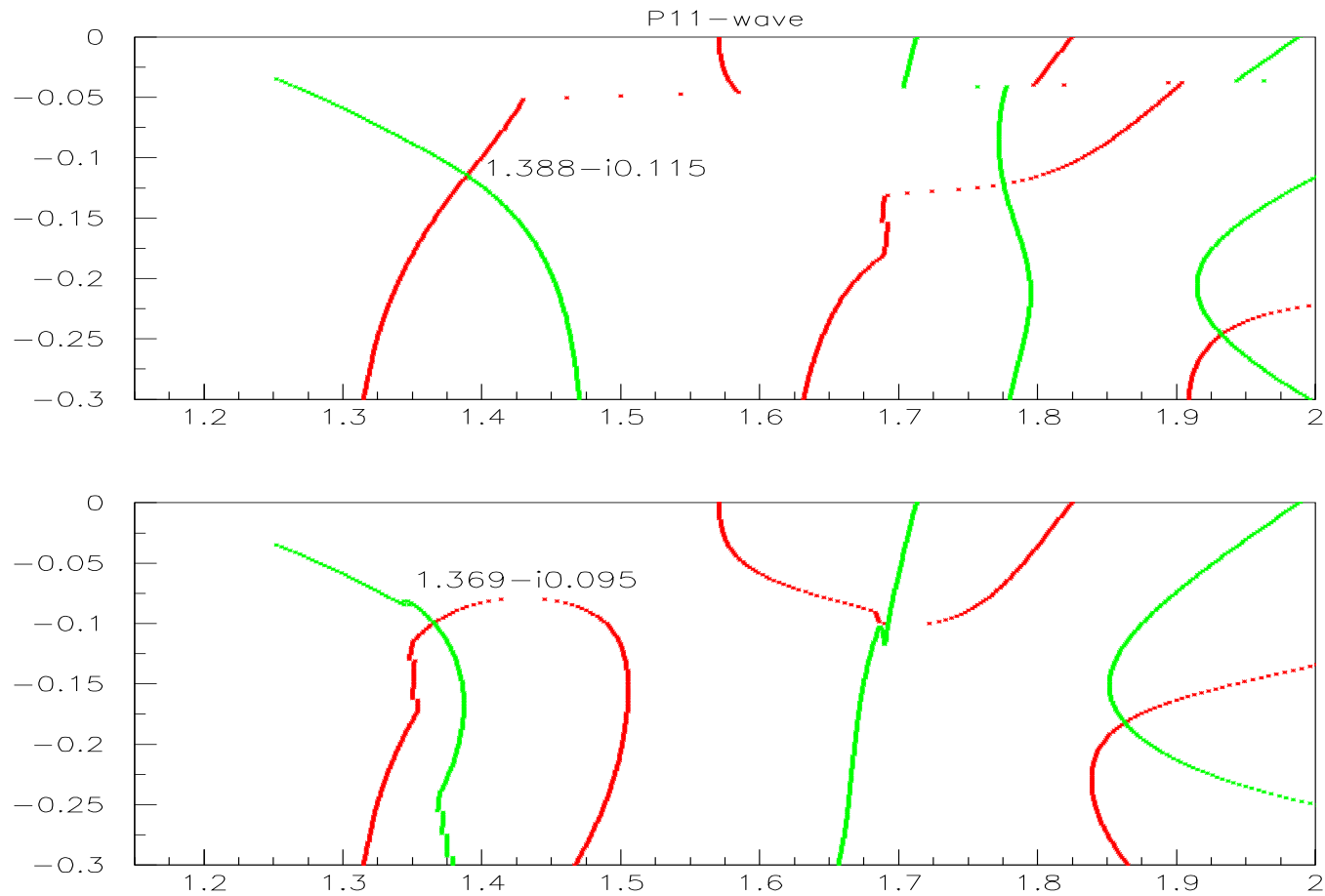


**T-matrix poles:**  $M = 1368 \pm 7$  MeV,  $2 Im = 190 \pm 10$  MeV;

$M = 1685 \pm 20$  MeV,  $2 Im = 160 \pm 45$  MeV

$M = 1870 \pm 30$  MeV,  $2 Im = 280 \pm 80$  MeV

**Position of zeros, for the determinant  $(I - i\rho K)^{-1}$ . Red points - real part and Green points -imaginary part.**



**Properties of  $N(1440)P_{11}$ . The left column lists mass, width, partial widths of the Breit-Wigner resonance; the right column pole position and squared couplings to the final state at the pole position.**

---



---

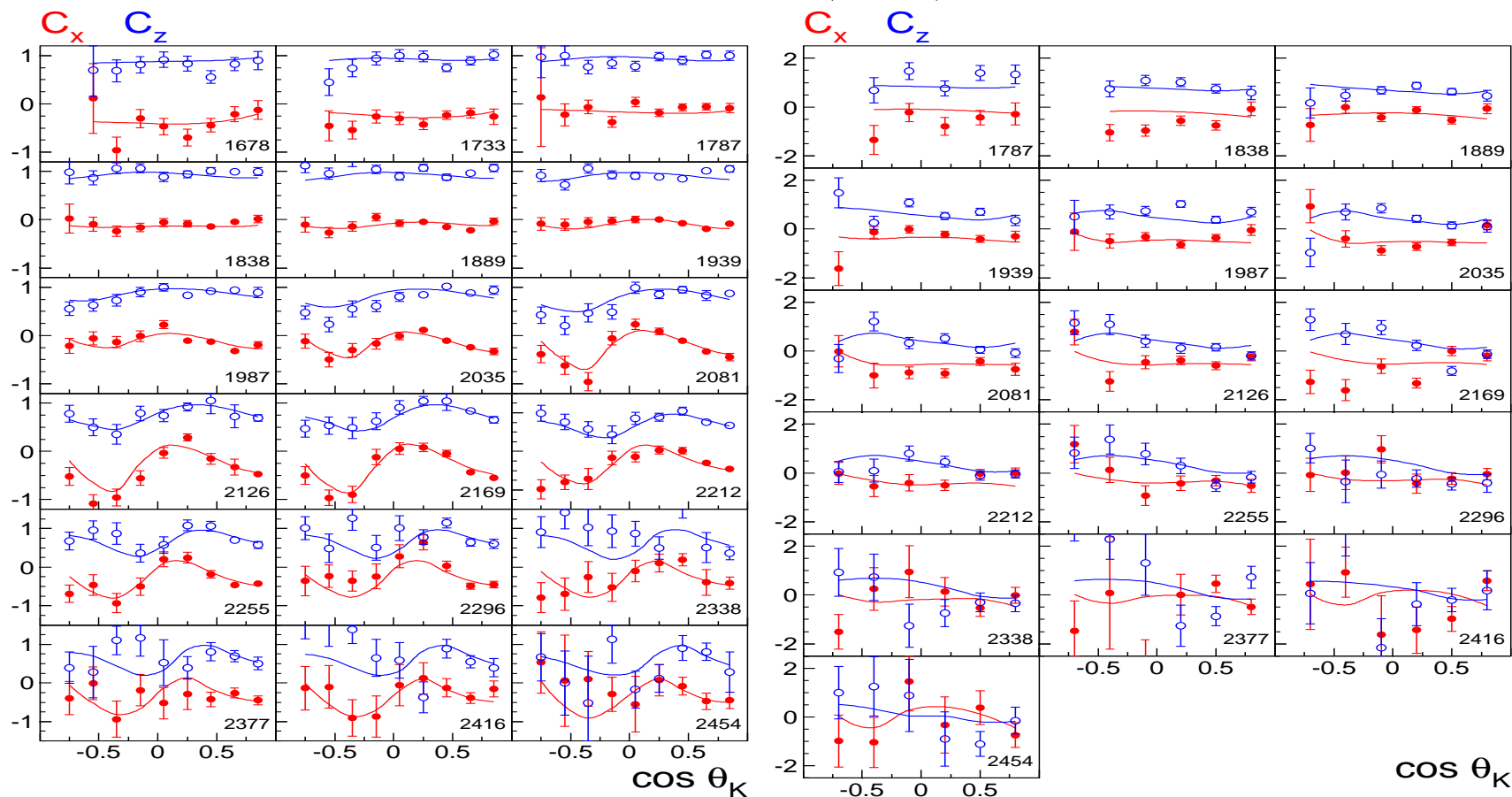
<b>M</b>	<b>=</b>	<b><math>1436 \pm 15 \text{ MeV}</math></b>	<b>M<sub>pole</sub></b>	<b>=</b>	<b><math>1371 \pm 7 \text{ MeV}</math></b>
<b><math>\Gamma</math></b>	<b>=</b>	<b><math>335 \pm 40 \text{ MeV}</math></b>	<b><math>\Gamma_{\text{pole}}</math></b>	<b>=</b>	<b><math>192 \pm 20 \text{ MeV}</math></b>
<b><math>\Gamma_{\pi N}</math></b>	<b>=</b>	<b><math>205 \pm 25 \text{ MeV}</math></b>	<b><math>g_{\pi N}</math></b>	<b>=</b>	<b><math>(0.51 \pm 0.05) \cdot e^{-i\pi \frac{(35 \pm 5)}{180}}</math></b>
<b><math>\Gamma_{\sigma N}</math></b>	<b>=</b>	<b><math>71 \pm 17 \text{ MeV}</math></b>	<b><math>g_{\sigma N}</math></b>	<b>=</b>	<b><math>(0.82 \pm 0.16) \cdot e^{-i\pi \frac{(20 \pm 13)}{180}}</math></b>
<b><math>\Gamma_{\pi \Delta}</math></b>	<b>=</b>	<b><math>59 \pm 15 \text{ MeV}</math></b>	<b><math>g_{\pi \Delta}</math></b>	<b>=</b>	<b><math>(-0.57 \pm 0.08) \cdot e^{i\pi \frac{(25 \pm 20)}{180}}</math></b>
<b>T-matrix:</b>		<b><math>A_{1/2} = 0.055 \pm 0.020 \text{ GeV}</math></b>	<b><math>\phi = (70 \pm 30)^\circ</math></b>		

---

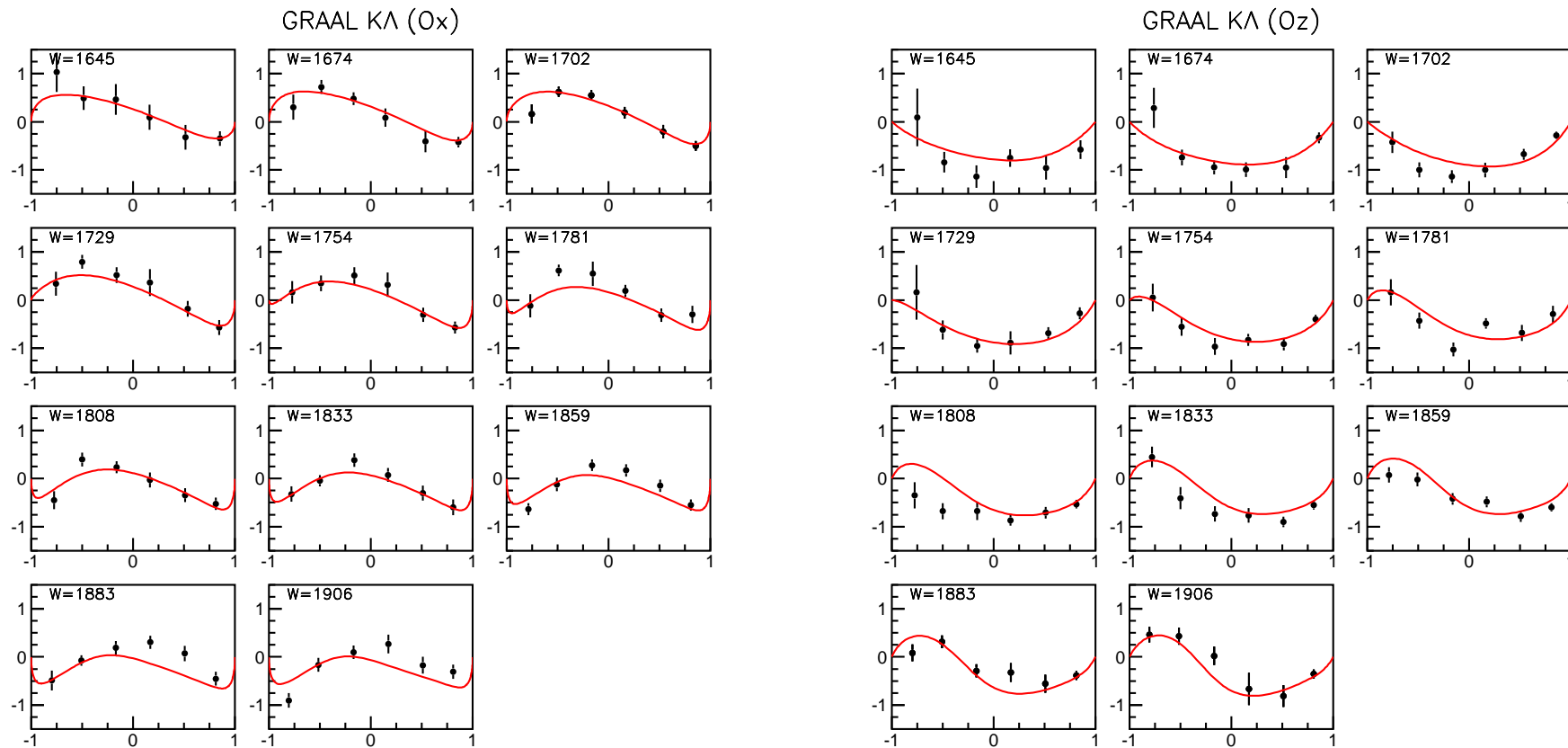


---

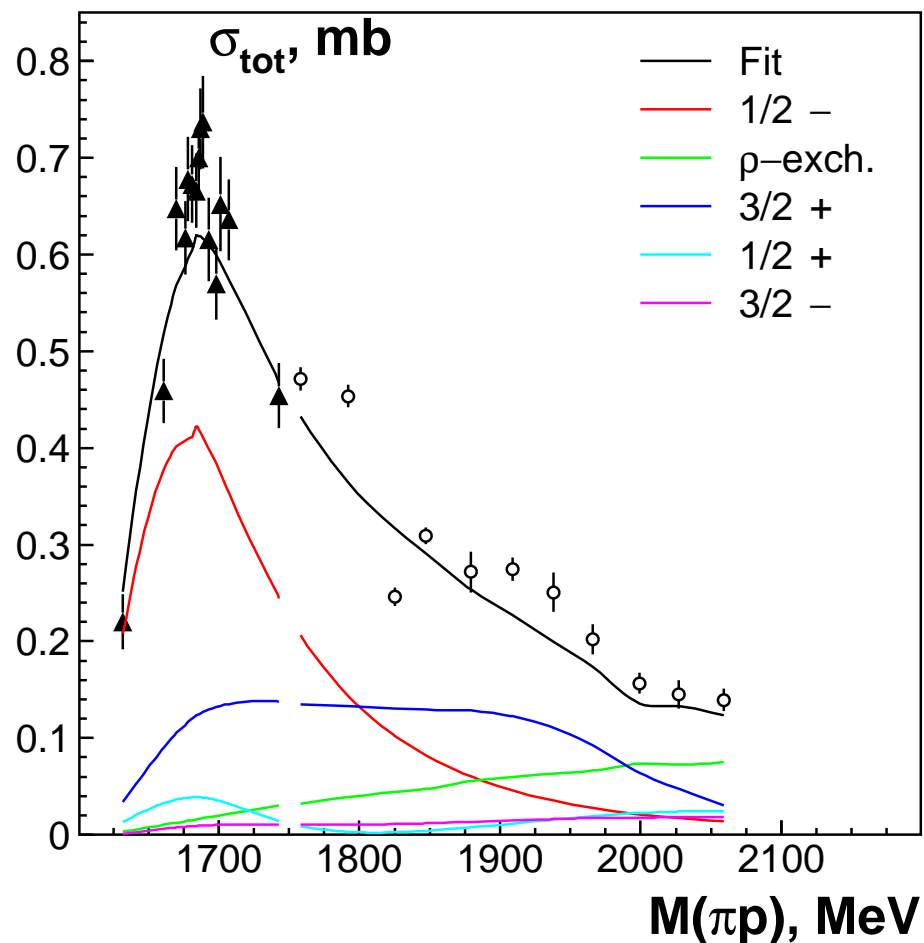
For  $\gamma p \rightarrow K\Lambda$  and  $\gamma p \rightarrow K\Sigma$  we have almost complete photoproduction experiment:  
 $\sigma$  (CLAS, SAPHIR),  $\Sigma$  (GRAAL, LEP),  $P$  (CLAS),  $C_x, C_z$  (CLAS),  $T, O_x, O_z$  (GRAAL).  
 The  $C_x$  and  $C_z$  data can be explained with  $P_{13}(1900)$ .



The solution is supported by the new GRALL data on  $O_x$   $O_z$  and  $T$ -observables: an important step to a complete experiment.



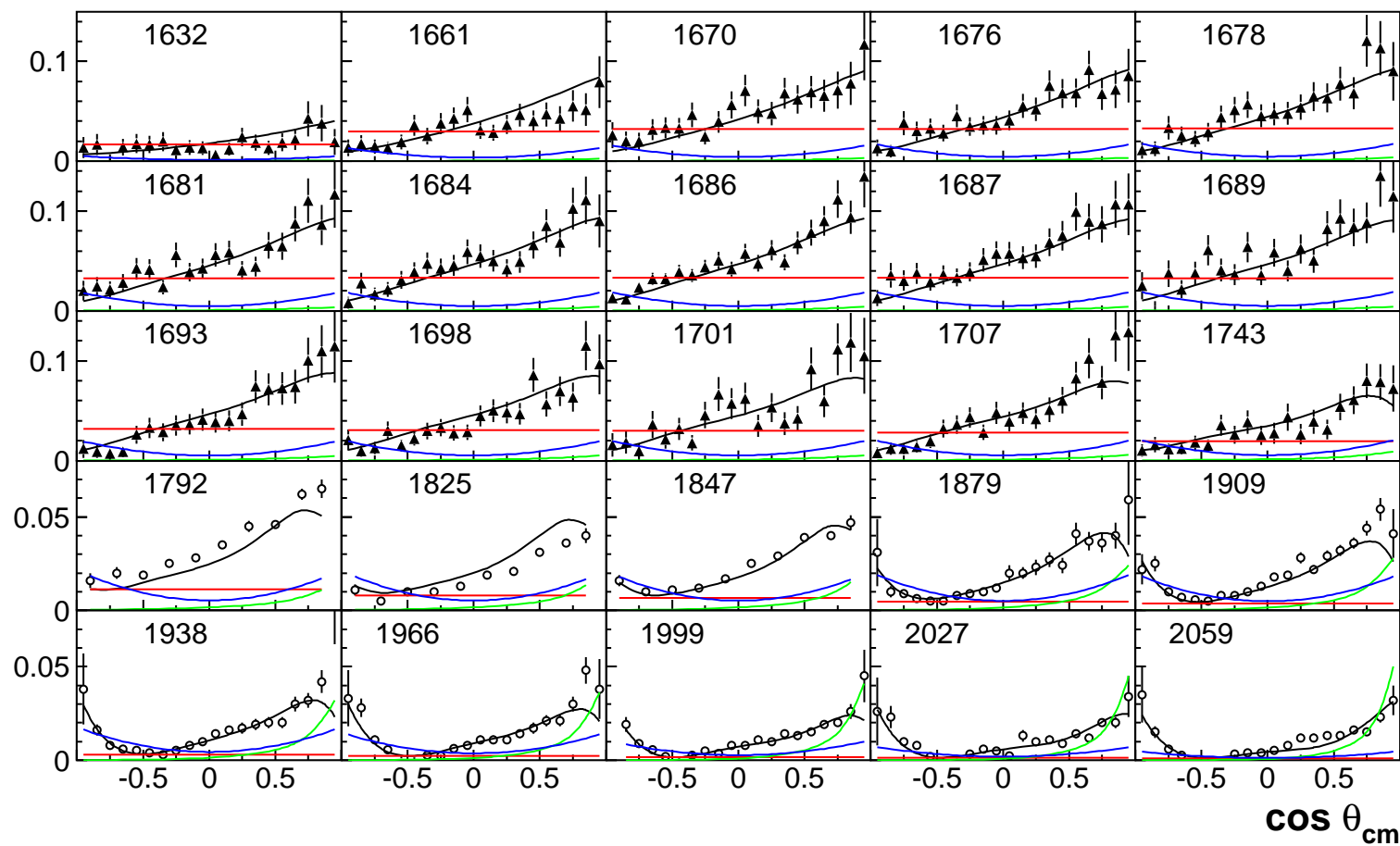
The total cross section for the  $\pi^- p \rightarrow K\Lambda$  reaction also shows a clear contribution from this state:



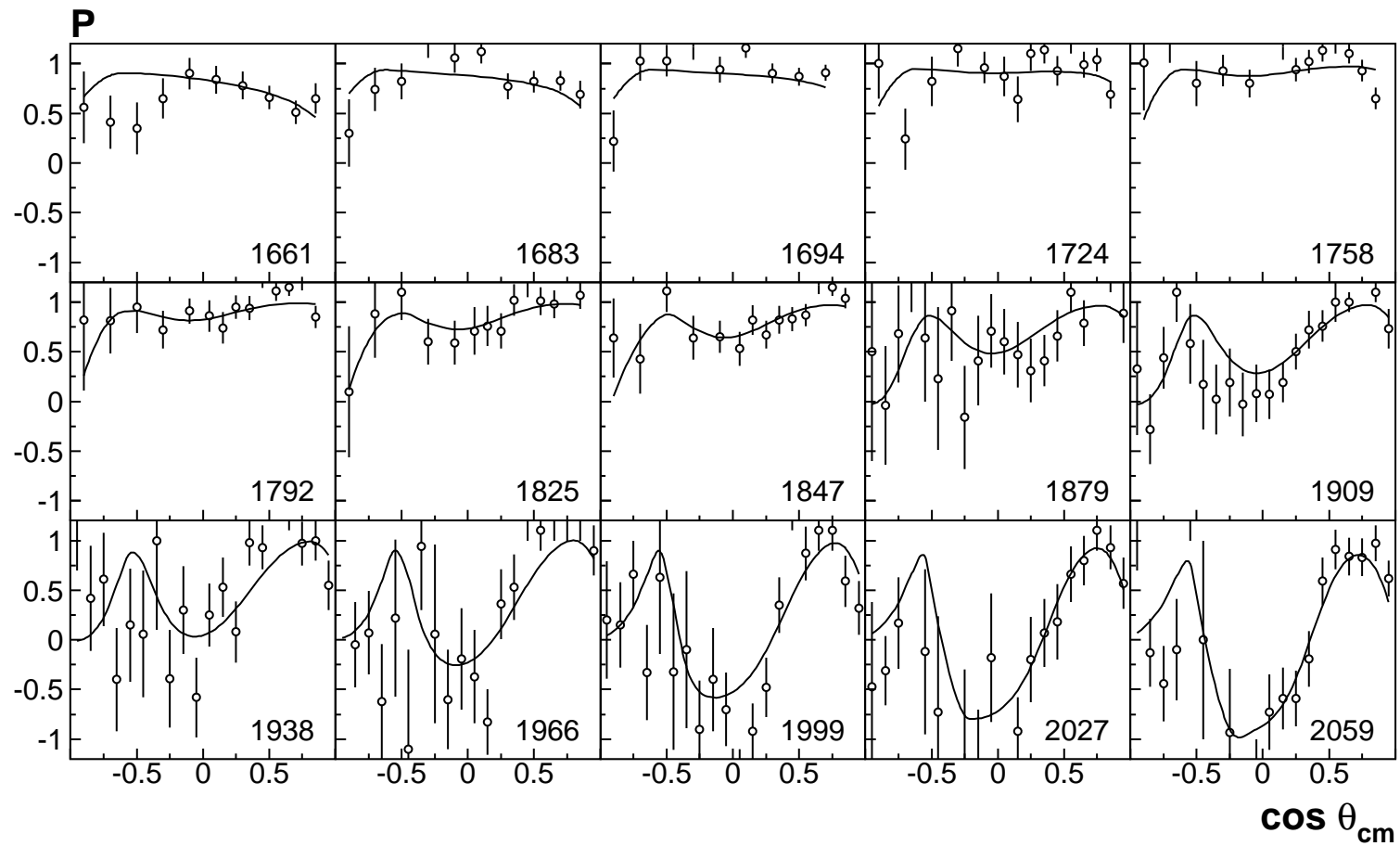
The same result was obtained before by the Giessen group:

V. Shklyar, H. Lenske, and U. Mosel, May 2005.

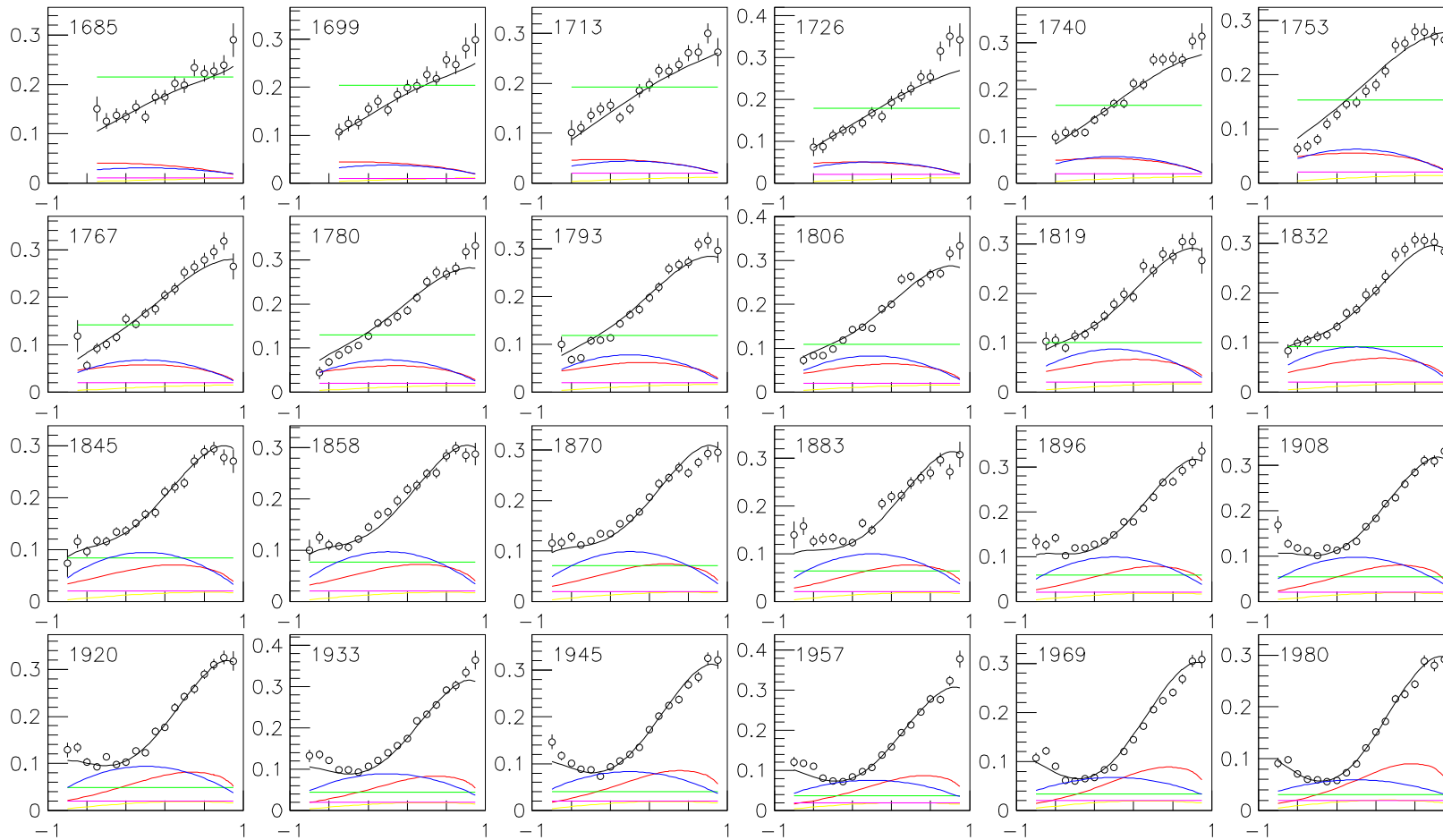
The differential cross section for the  $\pi^- p \rightarrow K \Lambda$  reaction. also shows a clear contribution from this state:

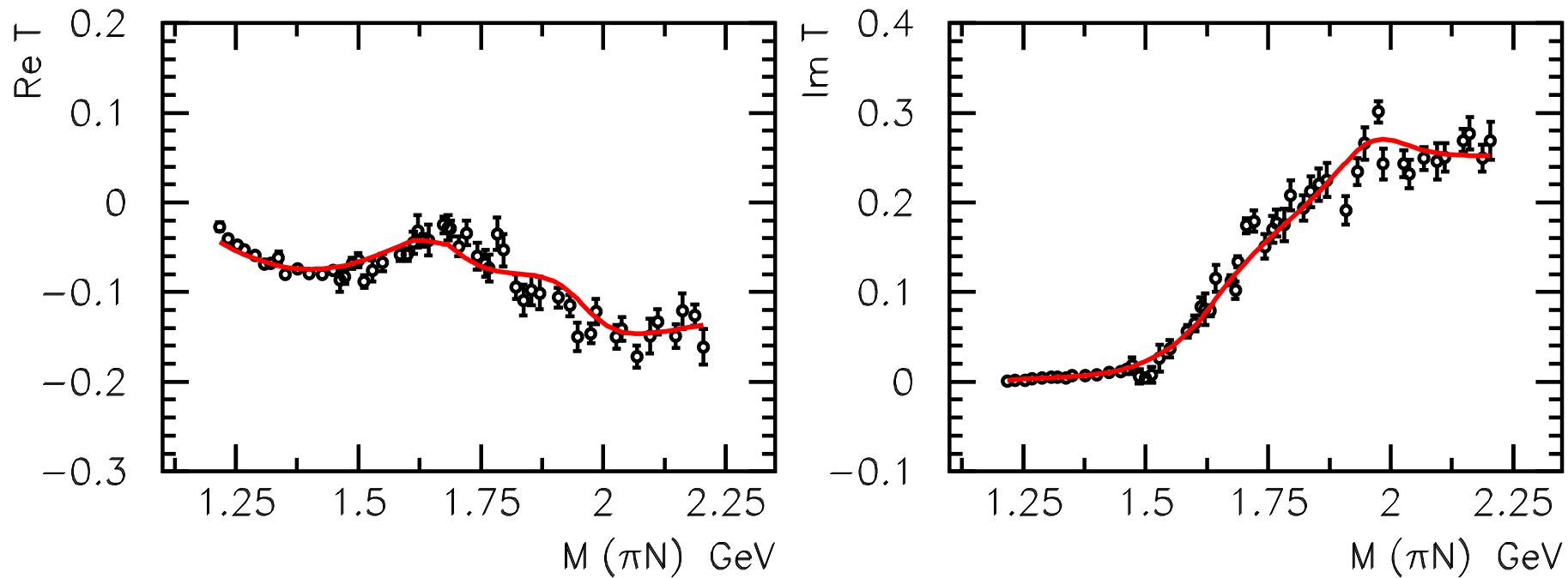


The recoil asymmetry for the  $\pi^- p \rightarrow K \Lambda$  reaction. also shows a clear contribution  
from this state:



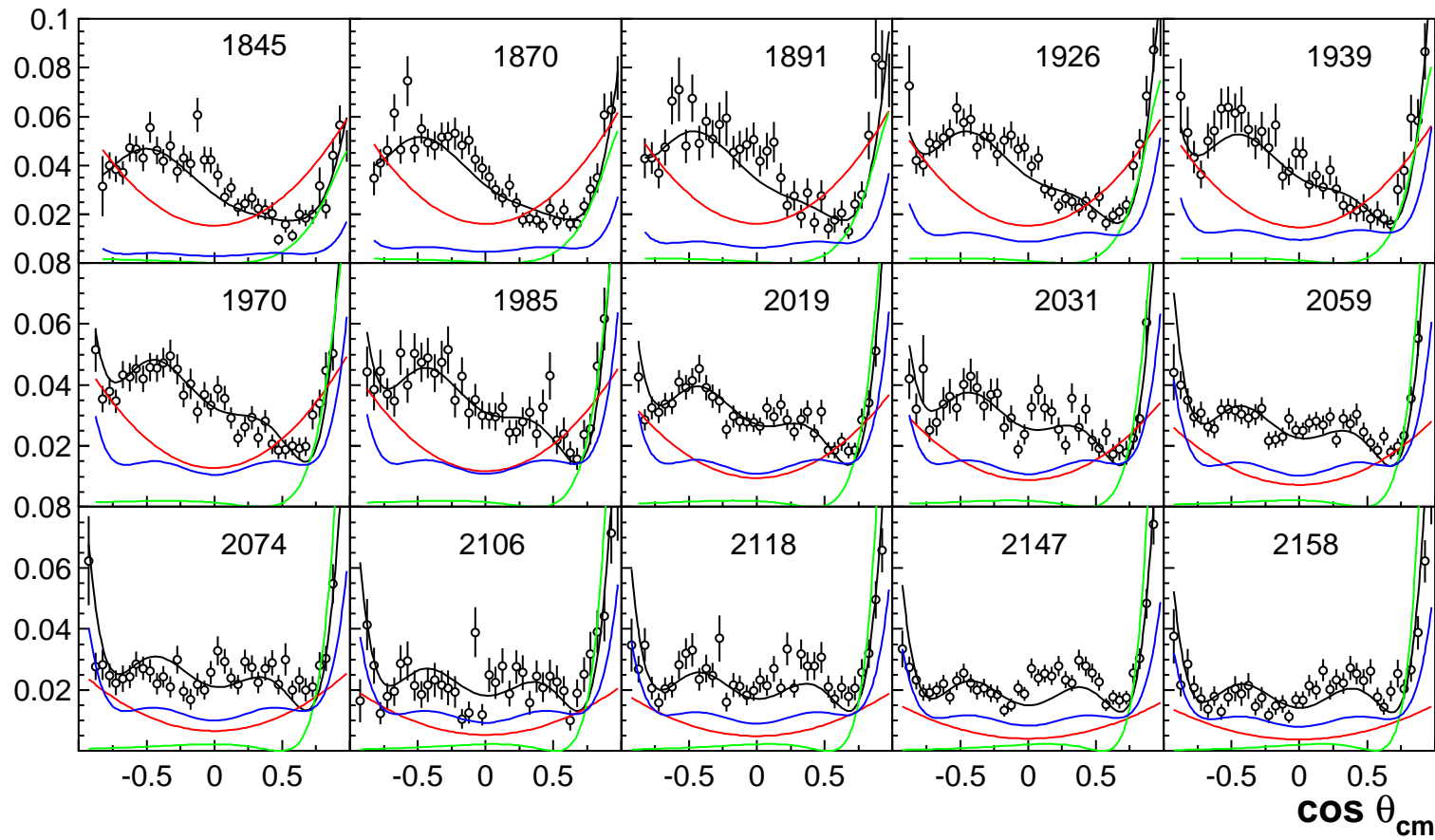
# The differential cross section for the $\gamma p \rightarrow K \Lambda$ reaction.



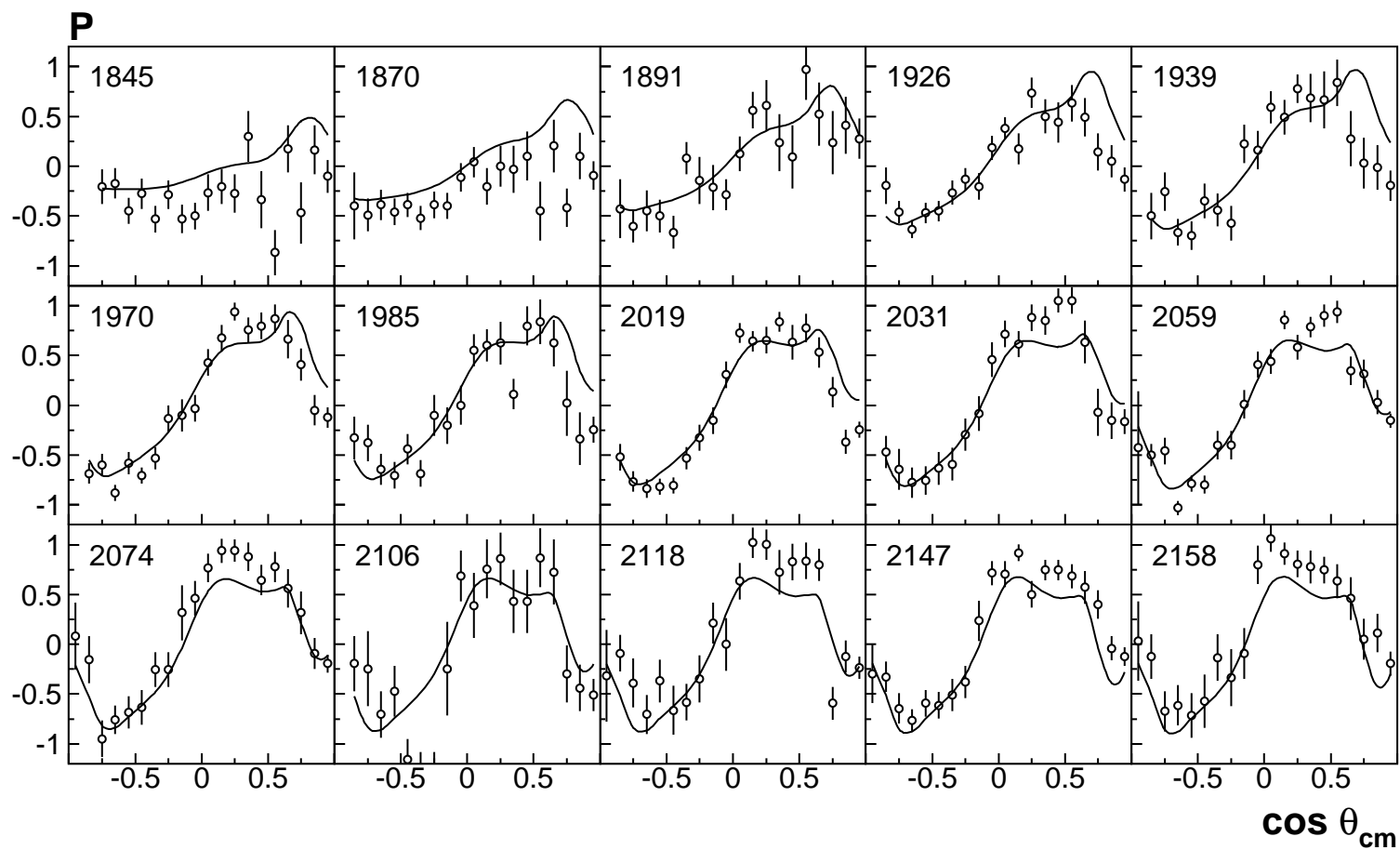
$N\pi \rightarrow N\pi$ ,  $P_{13}$  wave (3 pole 8 channel K-matrix)

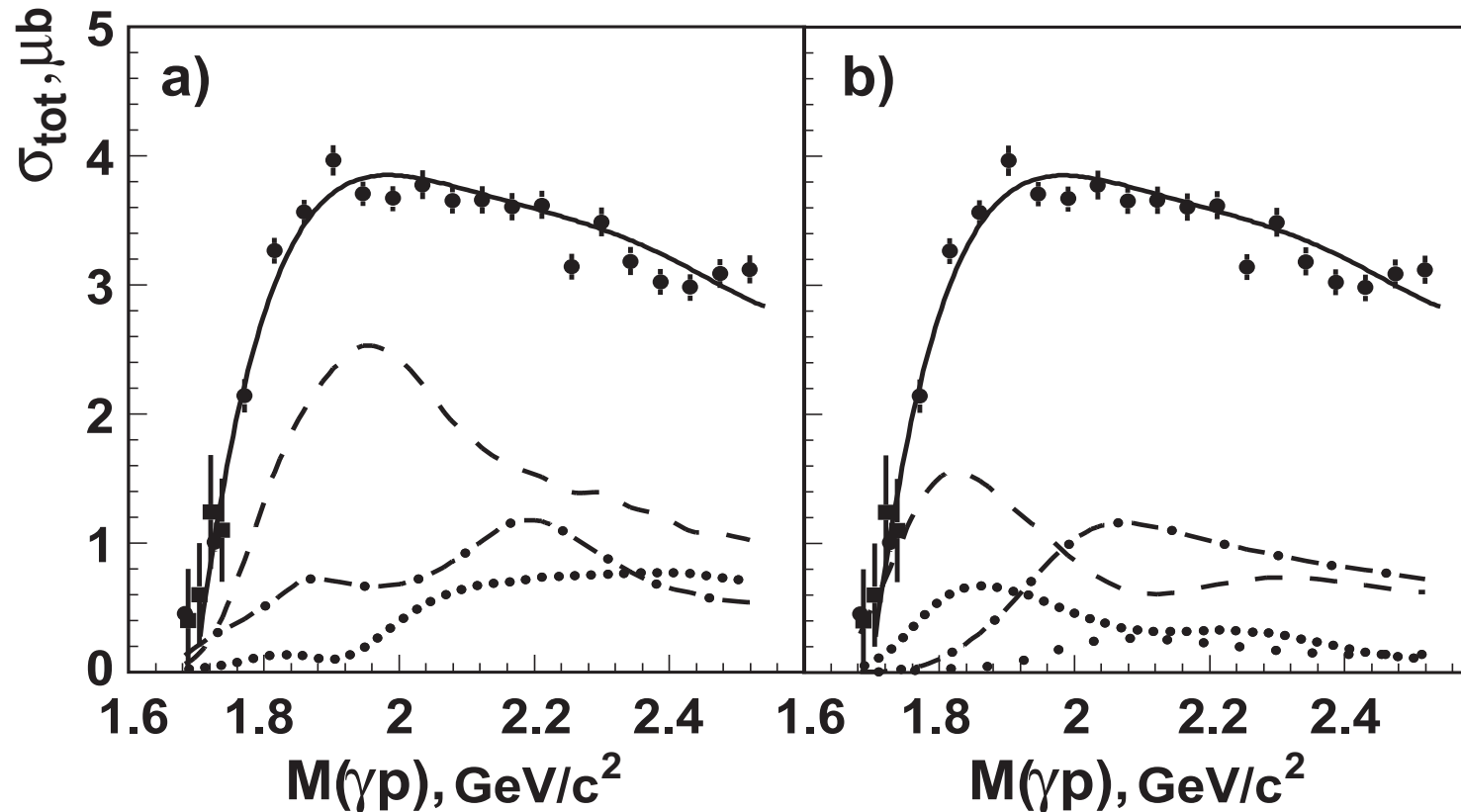
**2nd T-matrix poles:  $M = 1960 \pm 20$  MeV,  $2 \text{ Im} = 195 \pm 45$  MeV;**

The  $\Delta$ -states decaying into  $K\Sigma$  can be fixed from the  $\pi^+ \rightarrow K^+\Sigma$  data. The main contribution comes from  $P_{33}(1920)$  -red curves and  $F_{37}(1900)$  - blue curves.



The recoil asymmetry for the  $\pi^+ p \rightarrow K \Sigma$  reaction. also shows a clear contribution  
from this state:

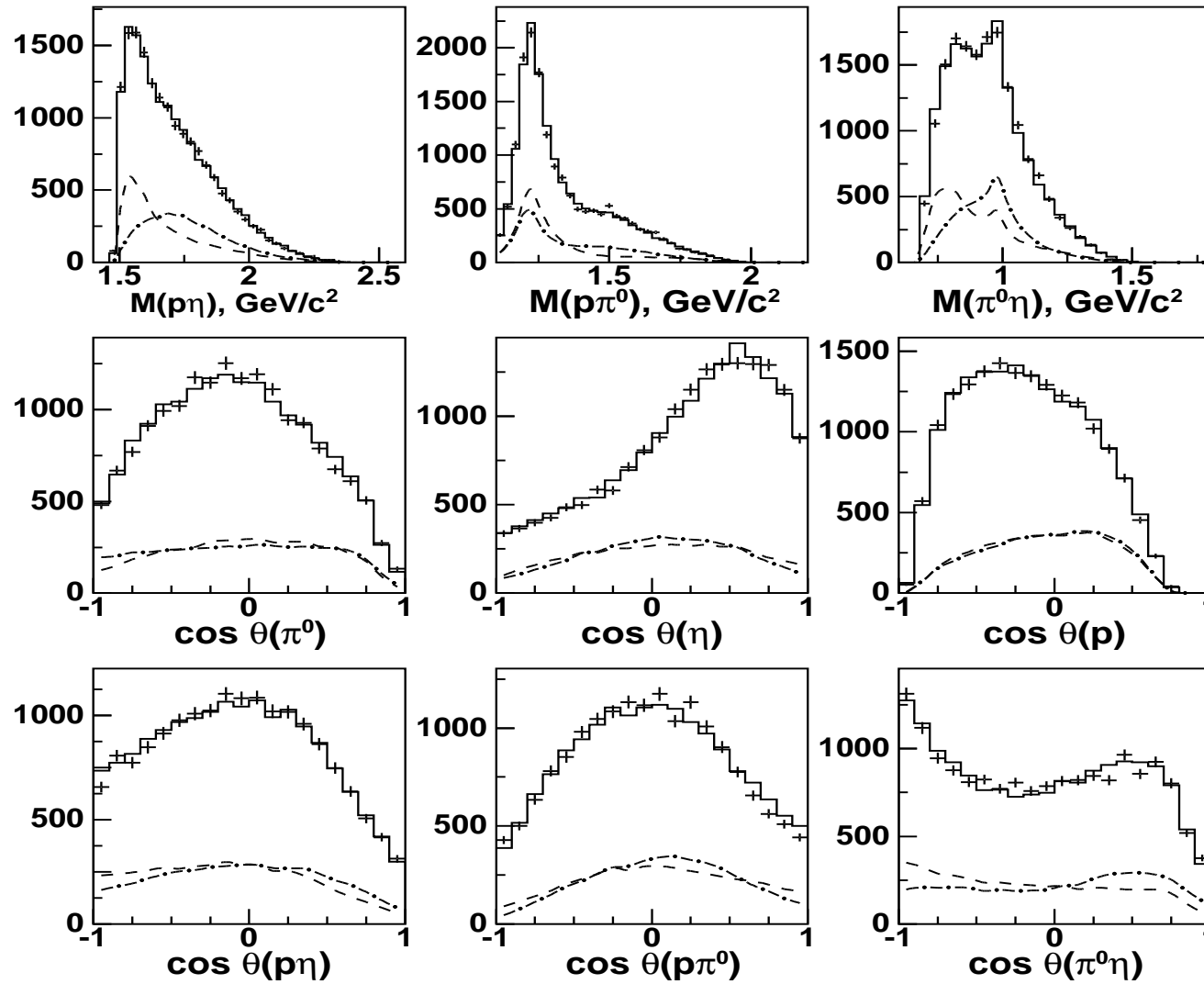


$$\gamma p \rightarrow p \pi^0 \eta \text{ (CB-ELSA)}$$


Left panel : contributions from  $\Delta(1232)\eta$  (dashed),  $S_{11}(1535)\pi$  (dashed-dotted) and  $N a_0(980)$  final states.

Right panel:  $D_{33}$  partial wave (dashed),  $P_{33}$  partial wave (dashed-dotted),  $D_{33} \rightarrow \Delta(1232)\eta$  (dotted) and  $D_{33} \rightarrow N a_0(980)$  (wide dotted).

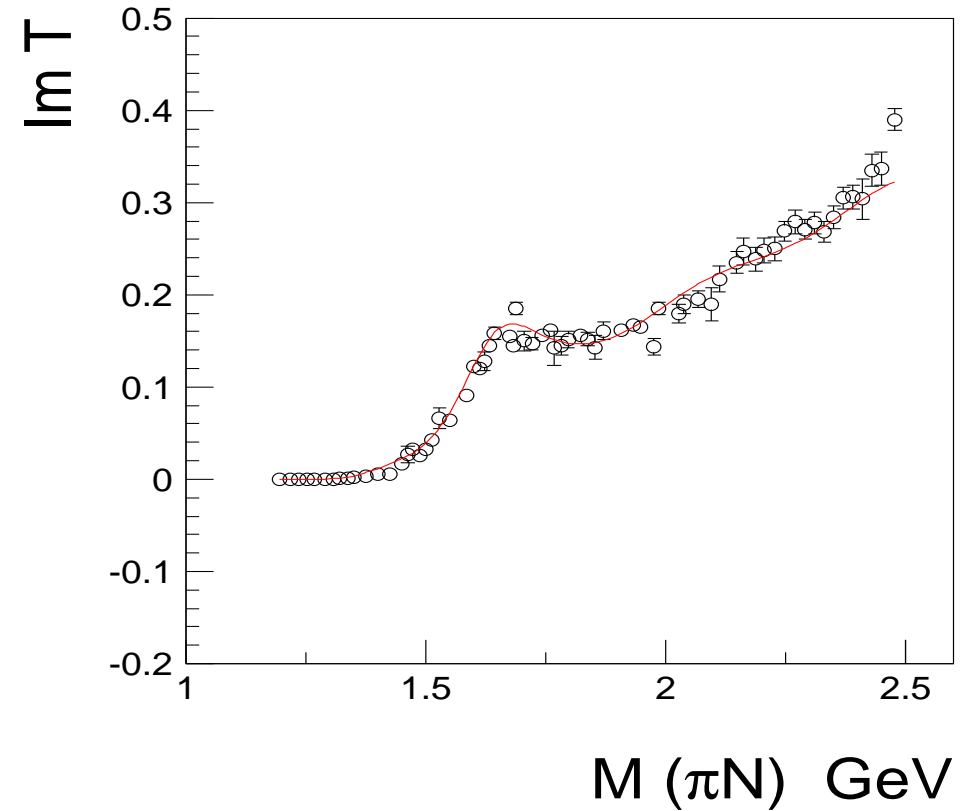
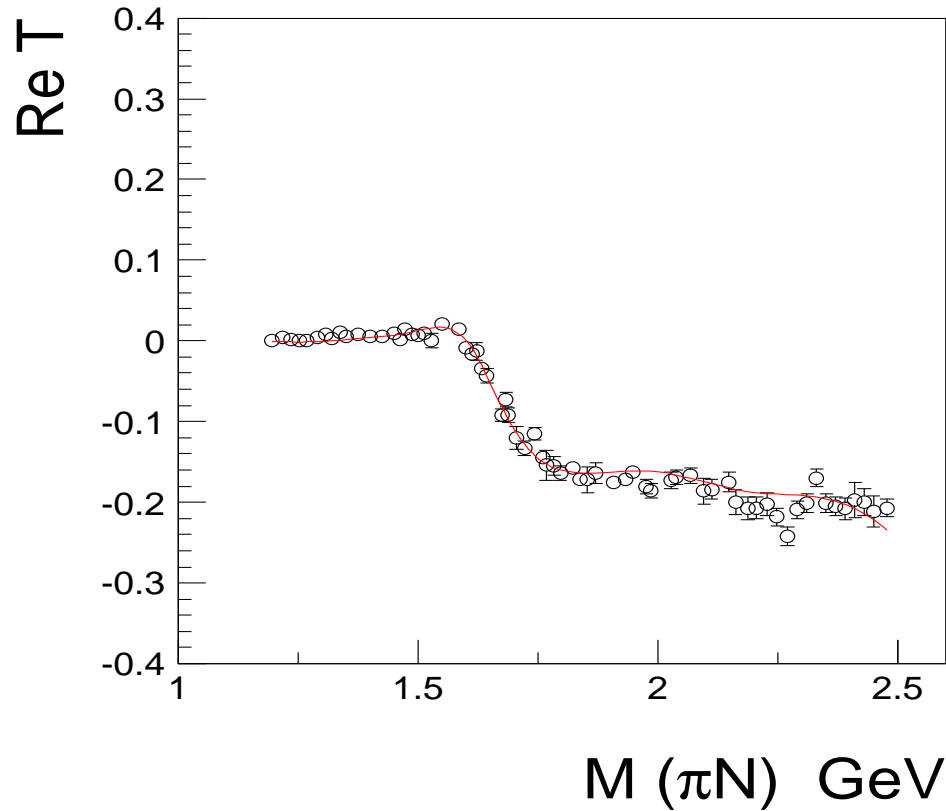
The  $\gamma p \rightarrow \pi^0 \eta p$  differential cross section for the total energy region.



# $N\pi \rightarrow N\pi$ $D_{33}$ wave (3 pole 5 channel K-matrix)

$D_{33}$

$D_{33}$



$D_{33}$ -wave:  $\pi N$ ,  $\Delta(1232)\pi$  ( $S$ - and  $D$ -waves),  $\Delta(1232)\eta$ ,  $S_{11}(1535)\pi$

**Properties of the  $\Delta(1920)P_{33}$  and  $\Delta(1940)D_{33}$  resonances.**

	$M_{pole}$	$\Gamma_{pole}$	$M_{BW}$	$\Gamma_{tot}^{BW}$
$\Delta(1920)P_{33}$	$1940 \pm 40$	$350^{+35}_{-55}$	$1970 \pm 35$	$375 \pm 50$
$\Delta(1940)D_{33}$	$1995 \pm 30$	$420 \pm 50$	$2000 \pm 40$	$410 \pm 70$
	$Br_{N\pi}$	$Br_{\Delta\eta}$	$Br_{N(1535)\pi}$	$Br_{Na_0(980)}$
$\Delta(1920)P_{33}$	$15 \pm 8$	$18 \pm 8$	$7 \pm 4$	$4 \pm 2$
$\Delta(1940)D_{33}$	$9 \pm 4$	$5 \pm 2$	$2 \pm 1$	$2 \pm 1$

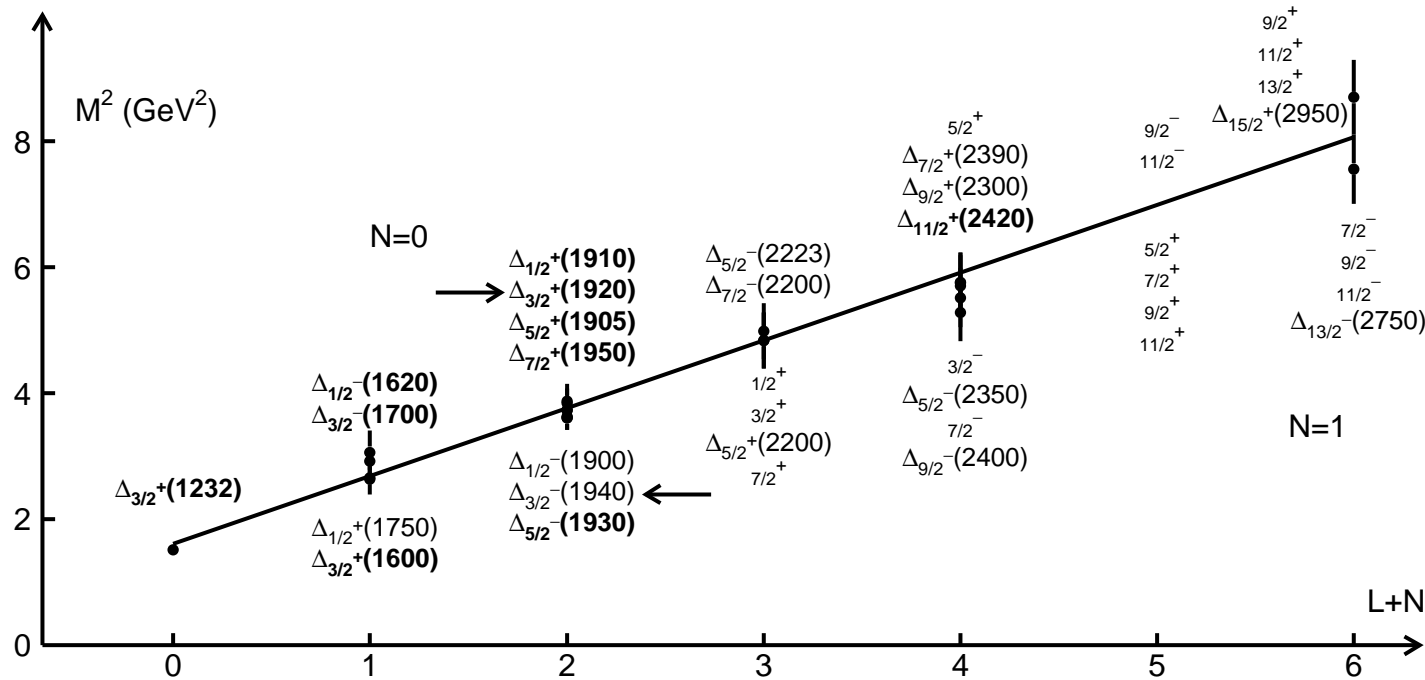
## Parity doublets of $N$ and $\Delta$ resonances at high mass region

Glozman suggested a restoration of chiral symmetry in high-mass excitations. Parity doublets must not interact by pion emission and could have a small coupling to  $\pi N$ .

$J=\frac{1}{2}$	$\mathbf{N}_{1/2+}$ (2100) <sup>a</sup> *	$\mathbf{N}_{1/2-}$ (2090) <sup>a</sup> *	$\Delta_{1/2+}$ (1910) ****	$\Delta_{1/2-}$ (1900) <sup>a</sup> **
$J=\frac{3}{2}$	$\mathbf{N}_{3/2+}$ (1900) <sup>a</sup> **	$\mathbf{N}_{3/2-}$ (2080) <sup>a</sup> **	$\Delta_{3/2+}$ (1920) <sup>a</sup> ***	$\Delta_{3/2-}$ (1940) <sup>a</sup> *
$J=\frac{5}{2}$	$\mathbf{N}_{5/2+}$ (2000) <sup>a</sup> **	$\mathbf{N}_{5/2-}$ (2200) <sup>a</sup> **	$\Delta_{5/2+}$ (1905) ****	$\Delta_{5/2-}$ (1930) <sup>a</sup> ***
$J=\frac{7}{2}$	$\mathbf{N}_{7/2+}$ (1990) <sup>a</sup> **	$\mathbf{N}_{7/2-}$ (2190) ****	$\Delta_{7/2+}$ (1950) ****	$\Delta_{7/2-}$ (2200) <sup>a</sup> *
$J=\frac{9}{2}$	$\mathbf{N}_{9/2+}$ (2220) ****	$\mathbf{N}_{9/2-}$ (2250) ****	$\Delta_{9/2+}$ (2300) **	$\Delta_{9/2-}$ (2400) <sup>a</sup> **
$J=\frac{3}{2}$	$\mathbf{N}_{3/2+}$ (1900)	$\mathbf{N}_{3/2-}$ (1875)	$\Delta_{3/2+}$ (1980)	$\Delta_{3/2-}$ (1985)
$J=\frac{5}{2}$	$\mathbf{N}_{5/2+}$ (1960)	$\mathbf{N}_{5/2-}$ (2070)	$\Delta_{5/2+}$ (1945)	$\Delta_{5/2-}$ (1930)
$J=\frac{7}{2}$	$\mathbf{N}_{7/2+}$ (1990)	$\mathbf{N}_{7/2-}$ (????)	$\Delta_{7/2+}$ (1910)	$\Delta_{7/2-}$ (????)

# Holographic QCD (AdS/QCD)

Soft-wall model prediction:  $M_{N,L}^2 = 4\lambda^2 \left( N + L + \frac{3}{2} \right)$



$$M_{N,L}^2 = 4\lambda^2 \left( N + L + \frac{3}{2} \right) - 2 \left( M_{\Delta}^2 - M_N^2 \right) \kappa_{gd}$$

$\kappa_{gd}$  is the fraction of most attractive color-antitriplet isosinglet diquark.

$\kappa_{gd}=0$  for  $\Delta$  and  $N(S=3/2)$  states,  $\frac{1}{2}$  for  $S = 1/2$  ( $70SU_6$ ) and  $\frac{1}{4}$  for  $S = 1/2$  ( $56SU_6$ ).

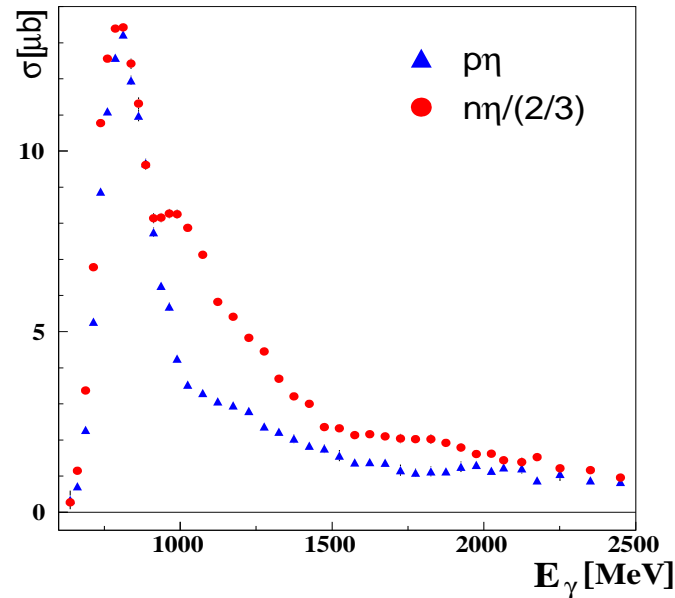
Hilmar Forkel and Eberhard Klempt, hep-ph:0810.2959v1

$L, S, N$	$\kappa_{gd}$	Resonance					Pred.
$0, \frac{1}{2}, 0$	$\frac{1}{2}$	$N(940)$				input:	<b>0.94</b>
$0, \frac{3}{2}, 0$	<b>0</b>	$\Delta(1232)$					<b>1.27</b>
$0, \frac{1}{2}, 1$	$\frac{1}{2}$	$N(1440)$					<b>1.40</b>
$1, \frac{1}{2}, 0$	$\frac{1}{4}$	$N(1535)$	$N(1520)$				<b>1.53</b>
$1, \frac{3}{2}, 0$	<b>0</b>	$N(1650)$	$N(1700)$	$N(1675)$			<b>1.64</b>
$1, \frac{1}{2}, 0$	<b>0</b>	$\Delta(1620)$	$\Delta(1700)$		$L, S, N=0, \frac{3}{2}, 1:$	$\Delta(1600)$	<b>1.64</b>
$2, \frac{1}{2}, 0$	$\frac{1}{2}$	$N(1720)$	$N(1680)$		$L, S, N=0, \frac{1}{2}, 2:$	$N(1710)$	<b>1.72</b>
$1, \frac{1}{2}, 1$	$\frac{1}{4}$	$N(????)$	$N(1875)$				<b>1.82</b>
$1, \frac{3}{2}, 1$	<b>0</b>	$\Delta(1900)$	$\Delta(1940)$	$\Delta(1930)$			<b>1.92</b>
$2, \frac{3}{2}, 0$	<b>0</b>	$\Delta(1910)$	$\Delta(1920)$	$\Delta(1905)$	$\Delta(1950)$		<b>1.92</b>
$2, \frac{3}{2}, 0$	<b>0</b>	$N(1880)$	$N(1900)$	$N(1990)$	$N(2000)$		<b>1.92</b>
$0, \frac{1}{2}, 3$	$\frac{1}{2}$	$N(2100)$					<b>2.03</b>
$3, \frac{1}{2}, 0$	$\frac{1}{4}$	$N(2070)$	$N(2190)$	$L, S, N=1, \frac{1}{2}, 2:$	$N(2080)$	$N(2090)$	<b>2.12</b>
$3, \frac{3}{2}, 0$	<b>0</b>	$N(2200)$	$N(2250)$	$L, S, N=1, \frac{1}{2}, 2:$	$\Delta(2223)$	$\Delta(2200)$	<b>2.20</b>
$4, \frac{1}{2}, 0$	$\frac{1}{2}$	$N(2220)$					<b>2.27</b>
$4, \frac{3}{2}, 0$	<b>0</b>	$\Delta(2390)$	$\Delta(2300)$	$\Delta(2420)$	$ L, N=3, 1:$	$\Delta(2400)$	<b>2.43</b>
$5, \frac{1}{2}, 0$	$\frac{1}{4}$	$N(2600)$			$ $	$\Delta(2350)$	<b>2.57</b>

## Summary

1. An approach for the combined analysis of the pion and photo induced reaction with two and multi particle final states is developed.
2. The combined analysis of more than 65 different reactions helped to identify the properties of known baryons.
3. The new data support the two new baryon states observed in hyperon photoproduction  $P_{11}(1880)$  and  $P_{13}(1900)$ .
4. The  $\eta$ -photoproduction data reveal the baryon resonance  $D_{15}(2070)$ .
5. The  $D_{33}(1940)$  state is needed for the description of the  $\gamma p \rightarrow \pi^0 \eta p$  data.
6. The data on  $\pi^- p \rightarrow \eta n$  and  $\pi^- p \rightarrow K^0 \Sigma$  support an existence of  $P_{11}(1710)$ .
7. The spectrum of observed states is in direct contradiction with a classical quark model. The best explanations are chiral symmetry restoration or AdS/QCD soft-wall model.

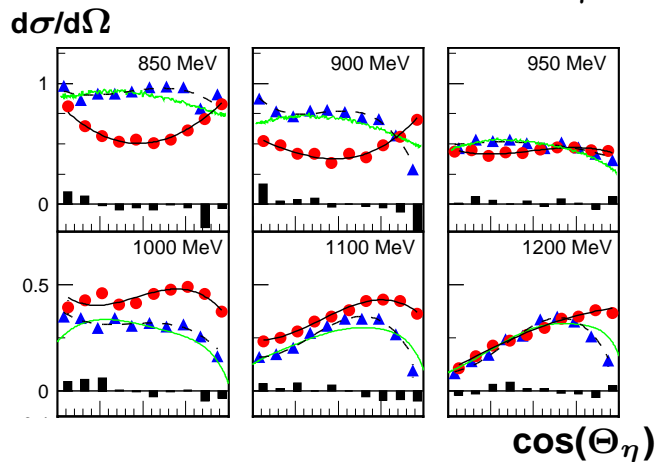
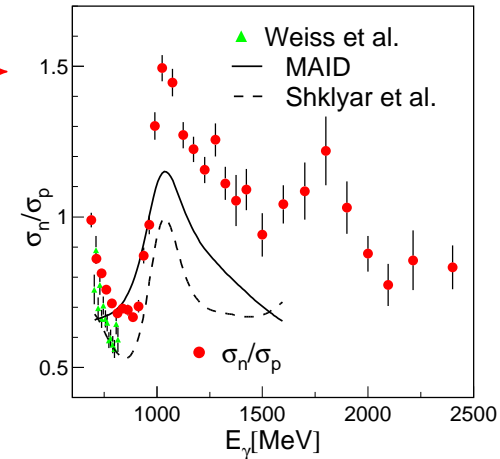
## $\eta$ -photoproduction at the neutron - CB-ELSA/TAPS data -



Investigation of  $\gamma d \rightarrow n\eta (p); \eta \rightarrow 3\pi^0$

$\leftrightarrow$  also CB-ELSA/TAPS data shows an enhancement around 1670 MeV (**preliminary**)

$\sigma_n / \sigma_p$   
data in comparison  
to MAID ( $\rightarrow$   
prediction  
 $\leftrightarrow$  effect of the  
 $D_{15}(1675)$



$\leftrightarrow$  something quite interesting going on

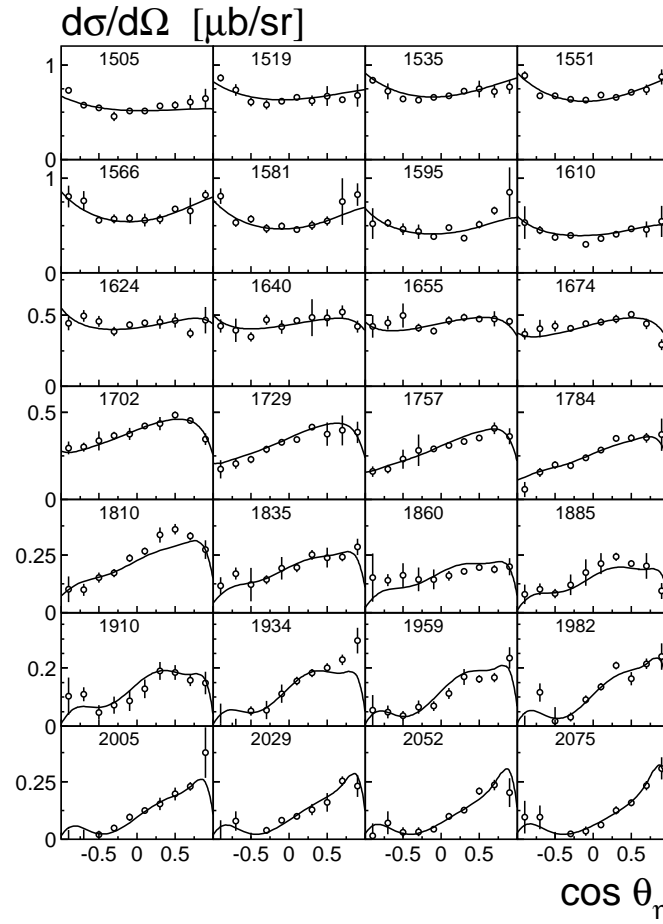
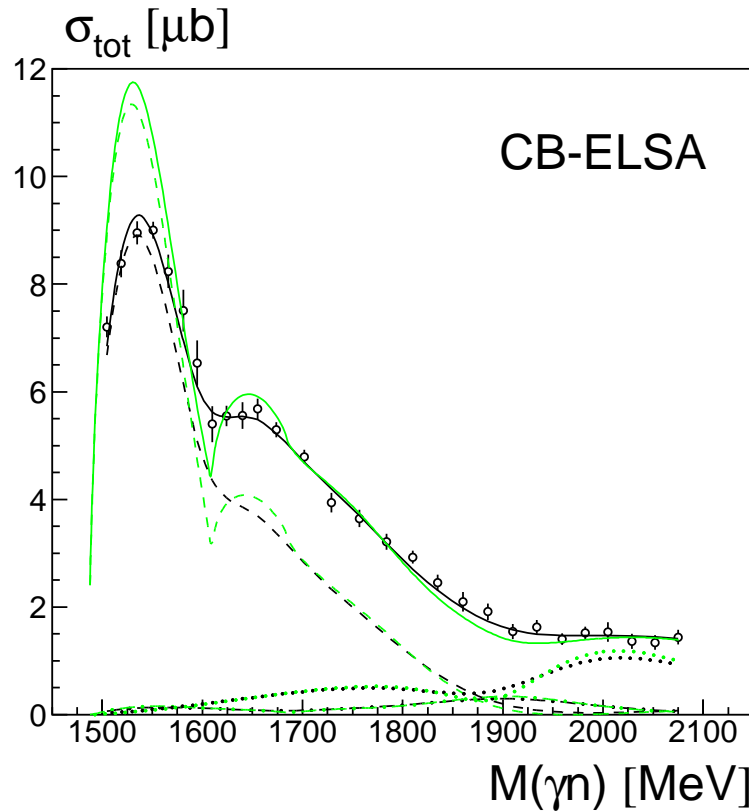
- role of the  $D_{15}(1675)$  ?
- narrow  $P_{11}(1670)$  ?
- explainable by  $S_{11}$ -states +  $P_{11}(1710)$  ?
- interference of  $S_{11}(1535)/S_{11}(1650)$  ?

$\leftrightarrow$  additional observables needed

### Three different class of solutions are found:

1. solutions with strong interference in  $S_{11}$  wave;
2. solutions with  $N(1710)P_{11}$  resonance;
3. solutions with narrow state in the mass region 1665 MeV.

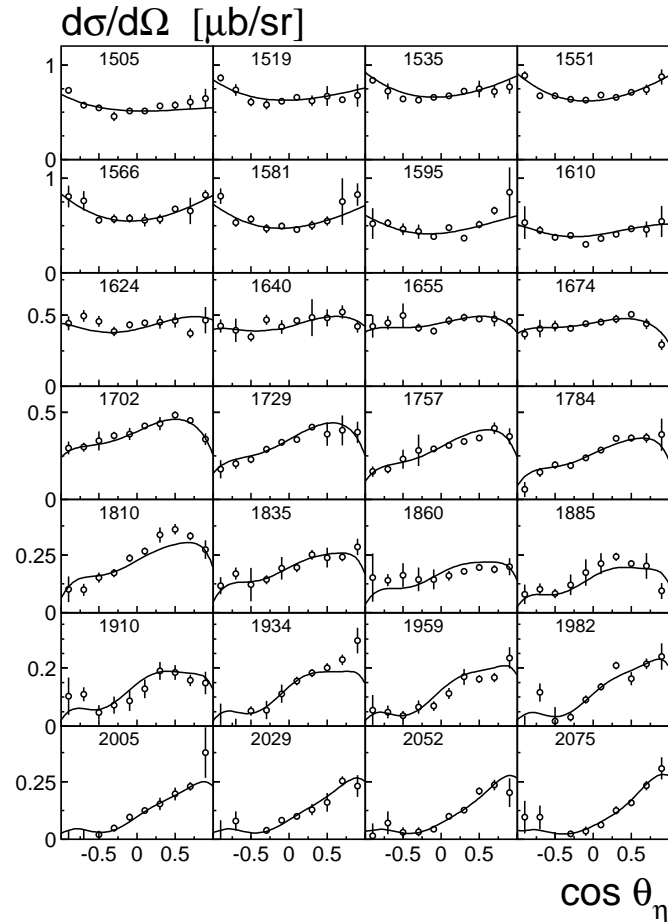
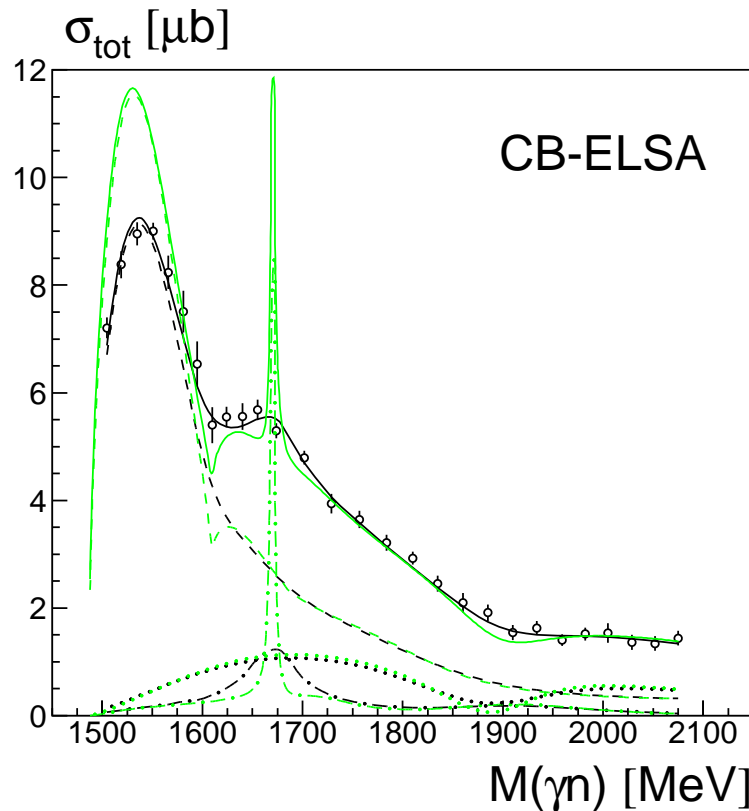
Observable	$N_{\text{data}}$	$\frac{\chi^2}{N_{\text{data}}}$	$\frac{\chi^2}{N_{\text{data}}}$	$\frac{\chi^2}{N_{\text{data}}}$	Ref.
		Sol. 1	Sol. 2	Sol. 3	
$\sigma(\gamma n \rightarrow n\eta)$	280	1.32	1.37	1.31	CB-ELSA
$\Sigma(\gamma n \rightarrow n\eta)$	88	1.75	2.07	1.79	GRAAL
$\sigma(\gamma n \rightarrow n\pi^0)$	147	2.01	2.48	2.03	SAID database
$\Sigma(\gamma n \rightarrow n\pi^0)$	28	1.02	0.95	0.90	GRAAL



The total and differential cross section for the reaction  $\gamma n \rightarrow \eta n$  obtained on the deuteron target.

The PWA result from the **solution with  $S_{11}$  interference (solution 1)** is shown. The **green curves** show the corresponding cross sections on the free neutron target (no Fermi motion).

Contributions:  $S_{11}$  (dashed),  $P_{13}$  (dotted) and  $P_{11}$  (dash-dotted)

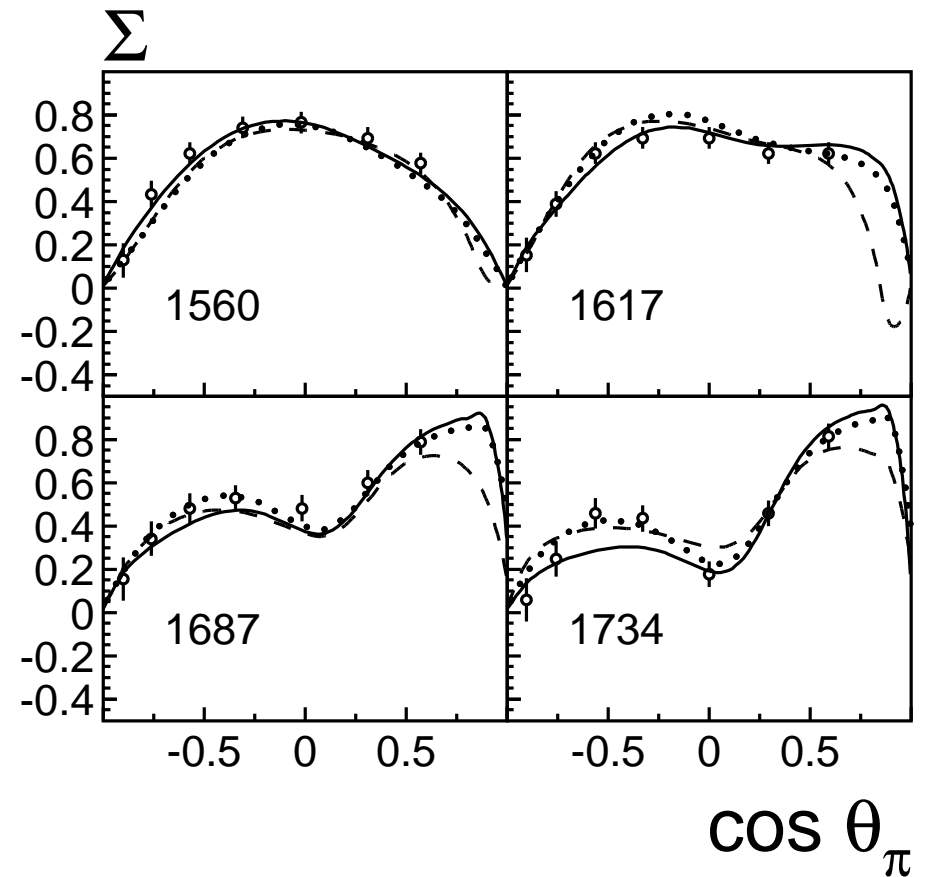
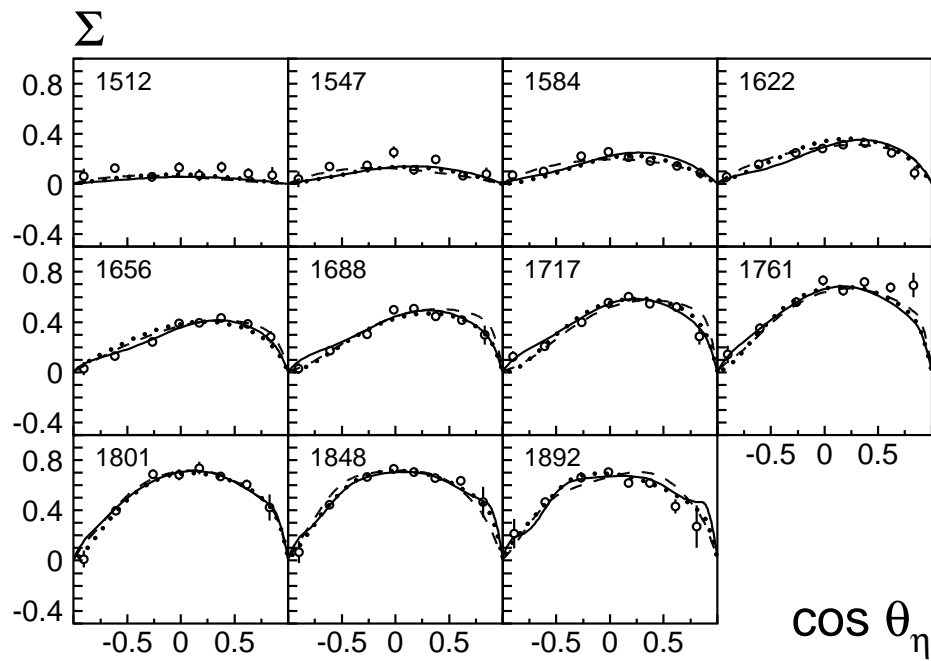


The total and differential cross section for the reaction  $\gamma n \rightarrow \eta n$  obtained on the deuteron target.

The PWA result from the **solution with narrow  $P_{11}$  resonance (solution 3)** is shown. The **green curves** show the corresponding cross sections on the free neutron target (no Fermi motion).

Contributions:  $S_{11}$  (dashed),  $P_{13}$  (dotted) and  $P_{11}$  (dash-dotted)

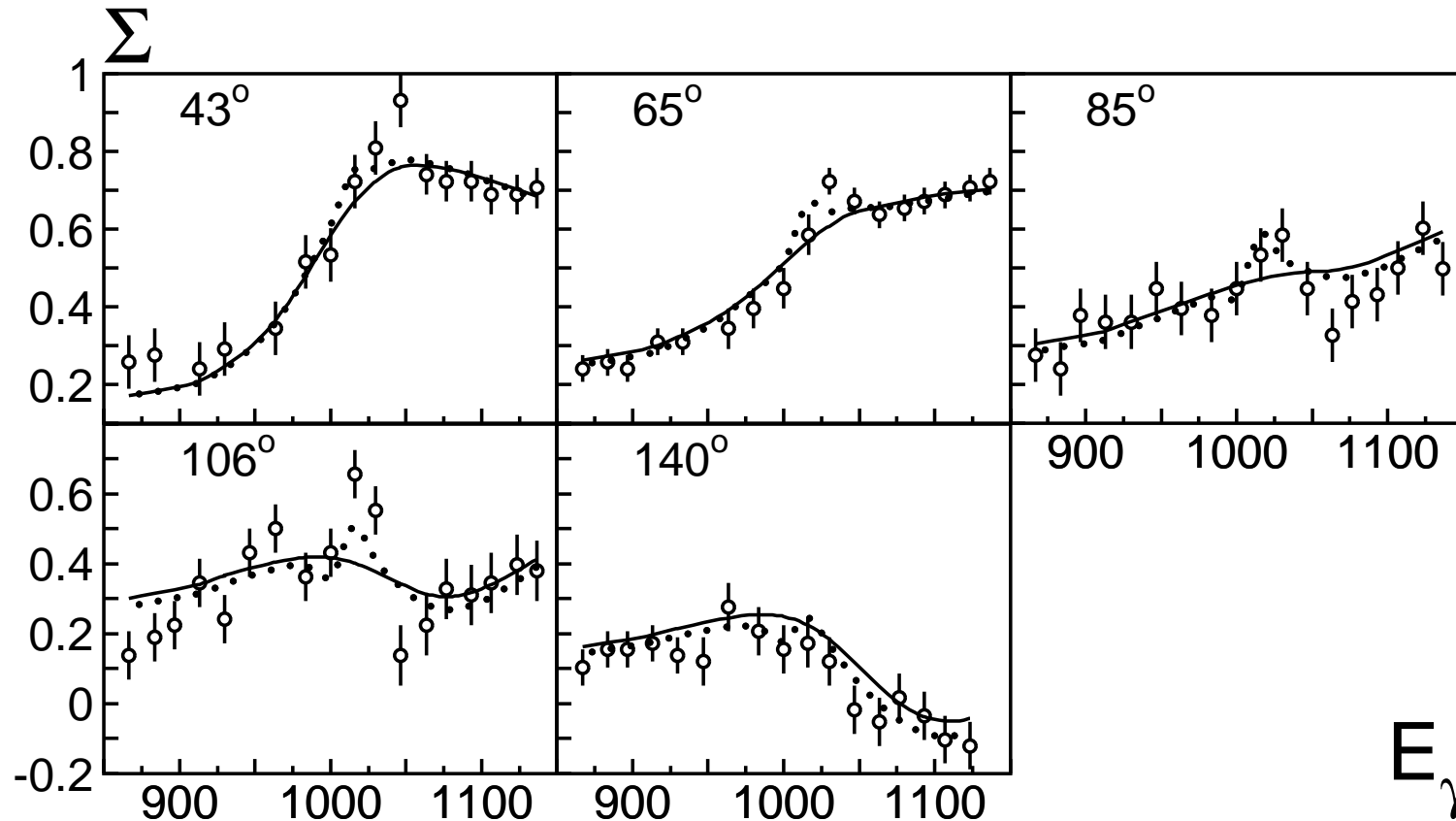
# Beam asymmetry for the $\gamma n \rightarrow \eta n$ and $\gamma n \rightarrow \pi^0 n$



# Beam asymmetry for the $\gamma p \rightarrow \eta p$ with fine bins

Solution 1:  $\chi^2 = 1.35$

Solution 3:  $\chi^2 = 0.95$



**The long-standing discrepancies between the photo-production amplitude  $A_{1/2}^n$  for  $N(1535)S_{11}$  production ( $A_{1/2}^n = -0.020 \pm 0.035 \text{ GeV}^{-1/2}$  from  $\gamma n \rightarrow n\pi^0$  (Arndt);  $A_{1/2}^n = -0.100 \pm 0.030 \text{ GeV}^{-1/2}$  from  $\gamma n \rightarrow n\eta$  (Krusche) is solved.**

	$S_{11}(1535)$	$S_{11}(1650)$
<b>Pole position (mass)</b>	$1.505 \pm 0.020$	$1.640 \pm 0.015$
<b>(width)</b>	$0.145 \pm 0.025$	$0.165 \pm 0.015$
<b>PDG</b>	$1.510 \pm 0.020$	$1.655 \pm 0.015$
	$0.170 \pm 0.080$	$0.165 \pm 0.015$
$A_{1/2}^p \text{ (GeV}^{-1/2}\text{)}$	$0.090 \pm 0.025$	$0.100 \pm 0.035$
<b>PDG</b>	$0.090 \pm 0.030$	$0.053 \pm 0.016$
<b>phase</b>	$(20 \pm 15)^\circ$	$(25 \pm 20)^\circ$
$A_{1/2}^n \text{ (GeV}^{-1/2}\text{)}$	$-0.080 \pm 0.020$	$-0.055 \pm 0.020$
<b>PDG</b>	$-0.046 \pm 0.027$	$-0.015 \pm 0.021$
<b>phase</b>	$(20 \pm 20)^\circ$	$(30 \pm 25)^\circ$